Loan Cy

UCRL 8330

UNIVERSITY OF CALIFORNIA

Radiation Laboratory

SURVEY OF TRITIUM-PRODUCING NUCLEAR REACTIONS

DISCLAIMER

UCRL-8330

UNIVERSITY OF CALIFORNIA

Radiation Laboratory
Berkeley, California

Contract No. W-7405-eng-48

SURVEY OF TRITIUM-PRODUCING NUCLEAR REACTIONS

José González-Vidal

(Thesis)

June, 1958

Printed for the U. S. Atomic Energy Commission

SURVEY OF TRITIUM-PRODUCING NUCLEAR REACTIONS

Contents

SURVEY OF TRITIUM-PRODUCING NUCLEAR REACTIONS

José González-Vidal

Radiation Laboratory and Department of Chemistry
University of California, Berkeley, California

June, 1958

ABSTRACT

(p,t), (d,t), and (α,t) reactions have been investigated throughout the periodic table by bombarding stacked metal foils and determining directly the tritium produced in the reaction. In the (α,t) reactions, there is conclusive evidence that most of the tritons are produced with high energies, thus indicating the presence of direct interaction processes. The curve representing the integrated cross-section vs Z of the target rises with decreasing Z; this, and the appearance of low-energy peaks in the individual excitation functions of low-Z targets indicate that at low and intermediate values of Z the relative number of low-energy tritons increases. These tritons are indicated to be the product of a compound-nucleus mechanism. For the (p,t) and (d,t) reactions the same compound-nucleus and direct-interaction effects are noticed.

The angular distributions of tritons from $Al^{27}(\alpha,t)Si^{28}$ and $Fe^{56}(\alpha,t)Co^{57}$ have been studied. It has been found that these angular distributions can be fitted by Butler's theory. The integrated differential cross-sections from these distributions account for a large portion of the cross-sections as determined by the stacked-foil technique.

SURVEY OF TRITIUM-PRODUCING NUCLEAR REACTIONS

INTRODUCTION

The study of spallation reactions produced by helium ions with energies up to 50 Mev in the heavy-element region of the periodic table has shown some very interesting features, especially in the $(\alpha,p2n)$ reaction.

Radiochemical investigations made with Th^{232},[1] U^{233},[2] U^{235},[3,4] U^{238},[5] Np^{237},[3] Pu^{238},[6,7] and Pu^{239} targets[6] show that the $(\alpha,p2n)$ reaction is, in general, the most prominent of the (α,xn) and (α,pxn) reactions. Furthermore it was observed that while for nonfissionable nuclides, such as lead,[8-10] the (α,xn) reactions were of greater abundance than the (α,pxn) reactions, for the fissionable nuclides the opposite is true; the magnitude of the (α,pxn) reactions remains approximately unchanged from lead to plutonium. Since it has been demonstrated, on the basis of the compound-nucleus mechanism, that the decrease of the (α,xn) reactions is due to fission competition,[6] it was suggested that the $(\alpha,p2n)$ reaction proceeds through a direct-interaction mechanism, leaving the residual heavy nucleus with such a low excitation energy that its subsequent fission is unlikely. Finally, with U^{238},[5] the product of the $(\alpha,p2n)$ reaction was observed at as low an energy as 22.6 Mev, whereas in this case the threshold for the production of one proton and two neutrons is 23.4 Mev. This observation led to the surmise that perhaps part of the cross section of the $(\alpha,p2n)$ is due to an (α,t) reaction, for which reaction the threshold is 14.4 Mev.

The foregoing considerations led to the hypothesis that at least part of the $(\alpha,p2n)$ cross-section was due to an (α,t) reaction that produces high-energy tritons. The following work was undertaken to test this hypothesis. By the direct observation of the tritons produced in the reaction and by the study of the angular distribution of the reaction products it was hoped to determine both the total contribution of the (α,t) reaction to the $(\alpha,p2n)$ reaction and the mechanism of the triton-

emitting process. It was also thought that the study of the (p,t), (d,t), and (α,t) reactions through the periodic table should be of interest, since such a study might help to better the understanding of the reaction mechanism.

So far only a few experiments on tritium emission have been described in the literature. Tritons from the (p,t), (d,t), and (α,t) reactions in bombardments with projectile energies greater than 100 Mev have been observed.[11-13] Currie, Libby, and Wolfgang determined the number of tritons produced from a number of elements by bombarding them with 450- and 2050-Mev protons.[14] With lower-energy particles (< 25 Mev), tritium production from deuteron and proton bombardments has been the subject of experimental investigation in both the region of the light elements,[15-18] and the region of heavy but not fissionable elements.[19]

EXPERIMENTAL PROCEDURE

A. Cross-Section Determinations

The method used for cross-section determinations was the bombardment of stacked metal foils with a beam of the desired particles. This was followed by heating of the foils in a measured amount of hydrogen carrier, selective diffusion of hydrogen isotopes through a palladium thimble, and introduction of the gas into a counter tube.

Metal Foils

For the helium-ion bombardments, 0.1-mm foils of natural Th^{232}, 0.05-mm foils of isotopically pure U^{238}, and 0.03-mm foils of natural magnesium, aluminum, titanium, iron, nickel, copper, zinc, silver, cadmium, indium, tin, platinum, gold, and lead were used. For cobalt and antimony, unavailable as foils, discs 3.0 mm thick were bombarded.

For the deuteron bombardments the same thicknesses and isotopic mixtures as above were used for aluminum, copper, zinc, silver, cadmium, tin, gold, lead, thorium, and uranium.

For the proton bombardments the same thicknesses and isotopic mixtures as in the previous cases were employed for thorium and uranium; but for aluminum, copper, zinc, silver, cadmium, indium, gold, and lead, foils 0.1-mm thick of the natural metals were used.

Since during bombardments there is likely to exist an appreciable neutron flux hitting the target, the metals were analyzed spectroscopically for interfering impurities, especially lithium. Impurities, when existent, were found to be negligible.

Bombardments

The helium-ion and deuteron bombardments were carried out by subjecting the targets to the external beam of the Crocker Laboratory 60-inch cyclotron. The proton bombardments were undertaken on the Berkeley linear accelerator. It will be shown that triton production by these three bombarding particles is quite general over the entire periodic table. For this reason it was impossible to vary the beam energy by placing degrading foils in front of the target without introducing an extraneous source of tritons. Thus, only maximum-energy beams were available to the first foil in the stack (48-Mev helium ions, 24-Mev deuterons, and 32 Mev protons).

The beam intensities employed were always less than 0.5 microampere.

Tritium-extraction apparatus

The apparatus used for tritium extraction is shown in Fig. 1. It is essentially the same as the one used by Currie, Libby, and Wolfgang.[14] The operation of the apparatus was as follows: the metal foil under investigation was placed in the Vycor tube; the apparatus was then evacuated and the tube filled with hydrogen to about 10 cm pressure. It was necessary to employ a carrier in order to have detectable pressure variations in the system. Hydrogen was used as the extractant because, unless it is present in excess, part of the tritium may remain in the target or possibly be trapped as hydroxide; furthermore, the use of a nonisotopic carrier would have thrown doubt on the completeness and reproducibility of

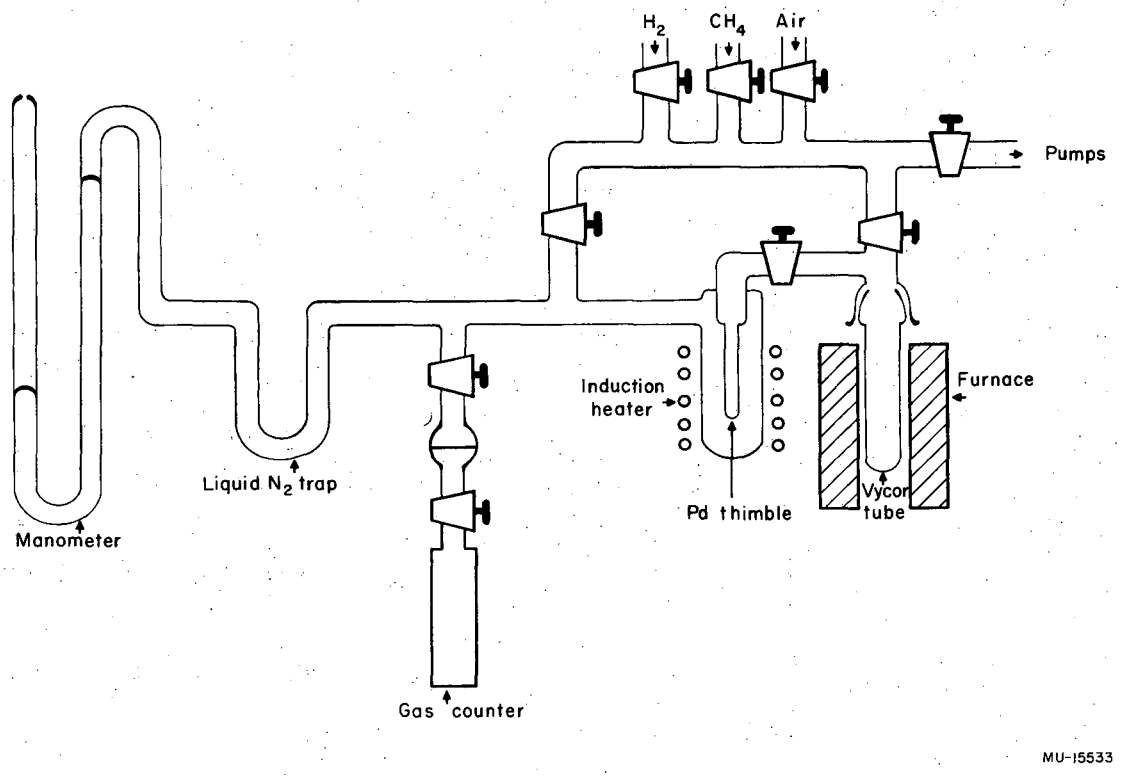

Fig. 1. Tritium extraction apparatus.

extraction. The tube was then heated to 1200°C (with low-melting-point metals the temperatures used were lower in order to avoid unnecessary vaporization of the metal). For metals that melted within the available temperature range, the heating times were 1 to 2 hours; for the rest of the cases heating times were longer: 4 to 8 hours. Next the hydrogen isotope mixtures were allowed to diffuse into the gas counter through a palladium thimble heated to about 500°C. Finally, the gas counter was filled to 1 atm. pressure with methane and counted in the "proportional" region.

Each of the gas counters was made of a section of cylindrical brass tubing 26 cm in length and 3.8 cm in outside diamter, with walls 0.79 cm thick. A stainless steel collector wire 0.0056 cm in diameter, ran along the axis of the cylinder.

The gas counters were calibrated against gas counters of very well-known characteristics at Livermore Laboratory. The calibration was carried out by filling both the counters used in this work and the Livermore counters to the same pressure with the same mixture of tritium, hydrogen, and methane and comparing the counting rates, with due regard to the volume differences. The Livermore counters had been previously calibrated against a known tritium sample from the National Bureau of Standards. The counting efficiency, C, of the counters used for these tritium determinations was found to be 0.87.

The counting voltage was 4100 volts. The proportional-region plateaus usually extended for 600 volts. It was found that the plateaus' widths remained essentially unchanged as long as the percentage of hydrogen in the counting-gas mixture was less than 10%.

Assuming the validity of Boyle's law, the tritium content per foil was given by

$$N_o = P_i V_v (1/C) N/P_f V_c ,$$

where N_o is the number of tritium disintegrations per minute originally in the foil, P_i is the hydrogen pressure originally present in the Vycor tube of the volume V_v, P_f is the final hydrogen pressure in the gas counter of volume V_c, and N is the number of counts per minute detected

in the counter. The volume of the gas counter was 190 cm^3, their effective volume 165 cm^3. The volume of the Vycor tube was 150 cm^3. The partial pressure of hydrogen in the counter tubes was ~0.04 atm. Counting rates varied from 2×10^2 to 1×10^5 counts per minute, representing a total yield of tritium from the target into the counter tubes of 35 to 40%.

The purpose of the palladium thimble was to separate tritium activities from other possible gaseous activities produced in the metal foil during bombardment: palladium membranes have the property of letting hydrogen isotopes through while acting as impermeable membranes toward other gases.[20] Even though this precaution was not necessary in many cases, it was always used as a measure of safety and for standardization purposes. The palladium thimble was heated to accelerate the diffision and to minimize hydrogen absorption by the metal. The palladium thimble was 10 cm long, 0.5 cm in diameter, and 0.05 mm thick.

The liquid nitrogen trap shown in Fig. 1 was used to condense mercury vapors proceeding from the manometer, which which were found to be harmful to the gas counter. Other cold traps (not shown in Fig. 1) were placed around the tubes connecting the vacuum system and the hydrogen and methane sources so as to condense any water vapor present in these gases.

The activity counted was that of tritium itself. It was identified as tritium both by its chemical property of diffusing through palladium and by its lack of decay (showing a half life greater than 5 years). Tritium is a 0.0180-Mev β^- emitter with a half life of 12.26 years.[21]

Sources of error

Several of the sources of error inherent in this system have been discussed by Currie, Libby, and Wolfgang.[14] Since their work was confined to proton-induced reactions at much higher energies, the relative importance of the errors is somewhat different from this.

The main sources of error are the following:

1. Secondary processes may produce tritium in the target during bombardment. Although this effect may be important at much higher energies, it should not be a factor in this work. There are two reasons:

first, they are second-order reactions, and second, the energies of the particles produced in nuclear reactions at these energies are not high enough, as a rule, to contribute significantly to triton emission.

2. Tritium may be lost from the target by virtue of its recoil energy. This possibility was circumvented by using enough foils to insure that the thickness of the stack was sufficient to cover the range of maximum-energy tritons.

3. Tritium may be lost by diffusion, since during the bombardment the beam heats the target. Precautions were taken against this danger by using beams of low intensity and by water-cooling the back of the target. Furthermore, several determinations using the same target material, different lengths of bombardment times, and different beam intensities gave reproducible results.

4. Diffusion of tritium from the target after bombardment may cause erroneous results. Wolfgang and Libby have shown this effect to be negligible for aluminum and beryllium and somewhat more important for nickel and iron.[22] This error was minimized by processing the targets soon after bombardment.

5. Extraction of tritium from the target may be incomplete. Wolfgang and Libby tested this by dissolving bombarded aluminum targets in acid and collecting the evolved hydrogen, as well as the hydrogen from the solution (by electrolysis), and thus found that the heat extraction, as described here, had removed 99% of the tritium.[22] During the investigations reported here, the efficiency of extraction was checked by submitting targets to two consecutive extractions; it was found that in every case the efficiency of the first operation was better than 98%.

6. The presence of tritium in the target material previous to bombardment could be a trivial source of error. This possibility was tested by submitting unbombarded metal foils to the tritium-extraction process. No tritium activity was found above counter background.

B. Angular Distributions

Triton angular-distribution measurements were confined to the two reactions $Al^{27}(\alpha,t)Si^{28}$ and $Fe^{56}(\alpha,t)Co^{57}$. The method employed for this phase of the investigation has already been discussed in great detail by Ellis,[23,24] Fischer,[25,26] Summers-Gill,[27,28] Vaughn,[29] and Knowles[30] and has since become standard procedure, therefore it will be only briefly described here.

Scattering chamber

The apparatus used was the scattering chamber at the Crocker Laboratory 60-inch cyclotron. This instrument receives the external beam of the cyclotron after the beam has been properly focused and collimated. The parget is placed in the center of the chamber, hanging from the lid. A particle detector, sitting on a rotating table on the bottom of the chamber, can be placed at any desired angle with respect to the beam. The target rests at 45° with respect to the beam.

The beam was measured with a Faraday cup placed at the back of the scattering chamber. The Faraday cup was provided with a foil wheel which was used to determine beam energies by range measurements. A CsI(Tl) crystal backed by a photomyltiplier tube was employed as a second monitor that counted elastically scattered helium-ions at a fixed angle with respect to the beam.

A schematic view of the apparatus is given in Fig. 2.

Targets

The targets were foils of natural aluminum and iron, 0.006-and 0.005-mm thick respectively. Natural aluminum is 100% Al^{27}, but natural iron is a mixture of isotopes; however, since Fe^{56} forms 91.6% of the mixture, all the detected tritons were assumed to proceed from the reactions of this nuclide.

Detector

The detector system was a range telescope. It consisted of three proportional chambers, as shown in Fig. 2. The first and second chambers

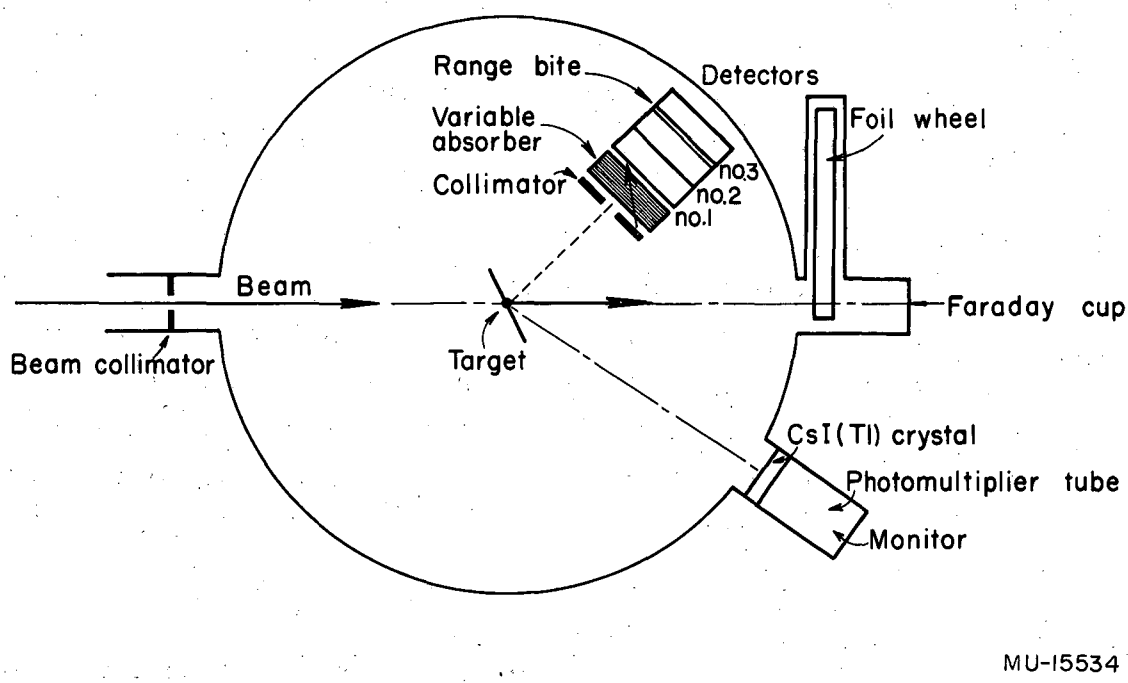

Fig. 2. Schematic diagram of scattering chamber and detector system.

formed a counter telescope and a pulse-height discriminator. Coincidence circuits registered coincidences in Chambers 1 and 2 (CC) and coincidences in Chambers 1, 2, and 3 (CCC). The difference, CC-CCC=CCA, gave the number of particles stopping in the aluminum window (range bite) between Chambers 2 and 3. This feature in conjunction with a system of variable absorbers in front of the counter permitted the detection of particles of any given range.

The detector opening was 0.6 cm in diameter and about 30 cm from the target, so that the angle of acceptance was about 1°.

Method of operation

The method of operation consisted of setting the discriminators for optimum detection of tritons. Then, since the range of the expected triton groups was known, the absorbers were changed in such a way as to cover the expected ranges and CCA counts taken at the desired absorber setting. For the discriminator settings used in this work the range bite was 3.3 mg of aluminum.

Limitations

Background limitations were quite severe. Even though the ratio of peak height to background can be improved by proper discriminator settings, it was found that in the best case the ratio was 1:2. The presence of this high background prevented the taking of differential cross sections beyond 60° with respect to the beam within a reasonable time.

The second limitation was the impossibility of attaining smaller angles than 7° with respect to the beam. The reason for this is that at small angles the detector gets in the path of the beam.

RESULTS

A. Cross-Section Determinations

As it was possible to use only maximum-energy beams for the bombardments, it was impossible to obtain true excitation functions, since -- owing to the long range of H^3 -- tritons found in one foil of the stack may have originated in a previous one (as will be shown). Cross sections for each foil were calculated on the basis of thin-target approximations, as if the beam were incident on each foil in which tritons were detected. Cross sections calculated in this way are only apparent cross sections. However, summation of these apparent cross sections over foil depth can be made to give the triton yield per incident bombarding particle by the use of the relationship

$$t/p = 6.02 \times 10^{-7} \frac{\rho}{A} \sum_{1}^{x(max)} \sigma_x \Delta_x ,$$

where t/p is the number of tritons produced in the reaction considered per incident particle, ρ is the number of atoms per cm^3 of target, A is the atomic weight of the target material, and σ_x (in millibarns) is the apparent cross section per foil of thickness Δ_x (in cm). The constant 6.02×10^{-7} takes care of unit conversions.

To avoid repetition, only a few representative graphs showing the variation of apparent cross section with target depth are shown (Figs. 3 to 12). Generally there appear on the abcissa of each graph three markings designated R, Q, and B. Point R indicates the end of the range of the incident beam, and Q and B indicate the range corresponding to the threshold of the reaction and the classical Coulomb barrier, respectively.

(p,t) cross-sections

Figures 3 to 5 show the variation of apparent cross-section vs target thickness for (p,t) reactions and elements in the light, medium, and heavy regions of the periodic table. The triton distributions are quite broad and all the tritium appears in foils where the beam has enough energy to overcome the Coulomb potential barrier and satisfy the threshold requirements of the reaction.

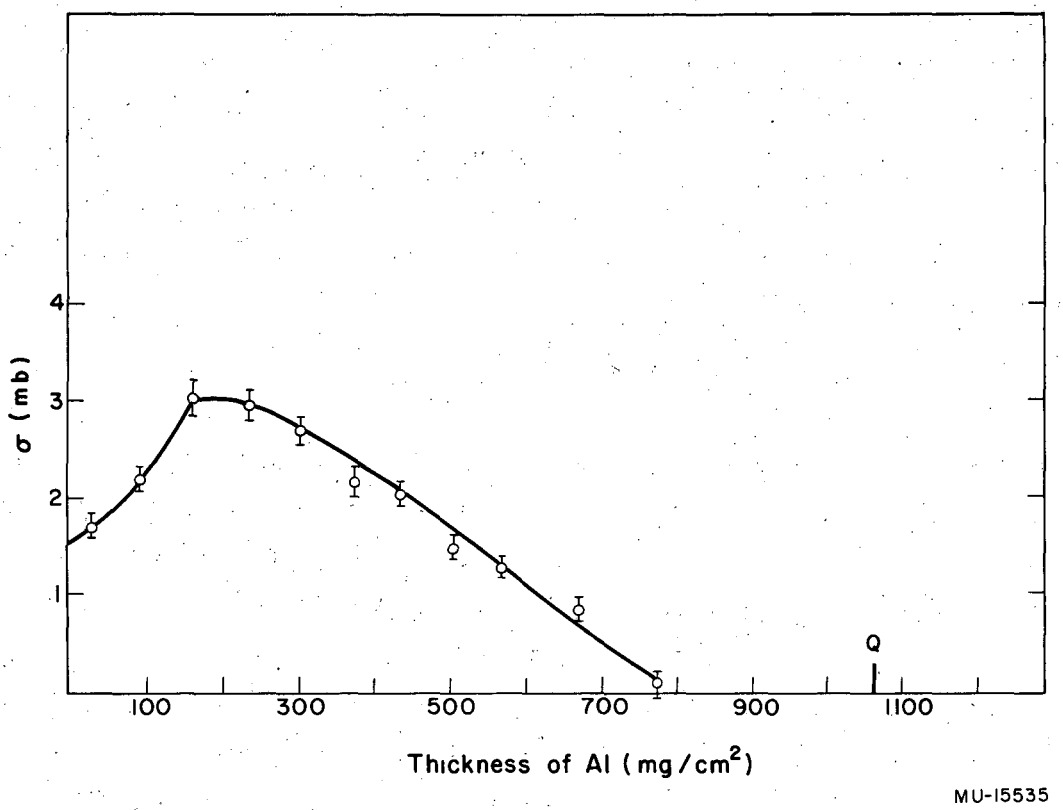

Fig. 3. Apparent excitation function for the $Al^{27}(p,t)Al^{25}$ reaction.

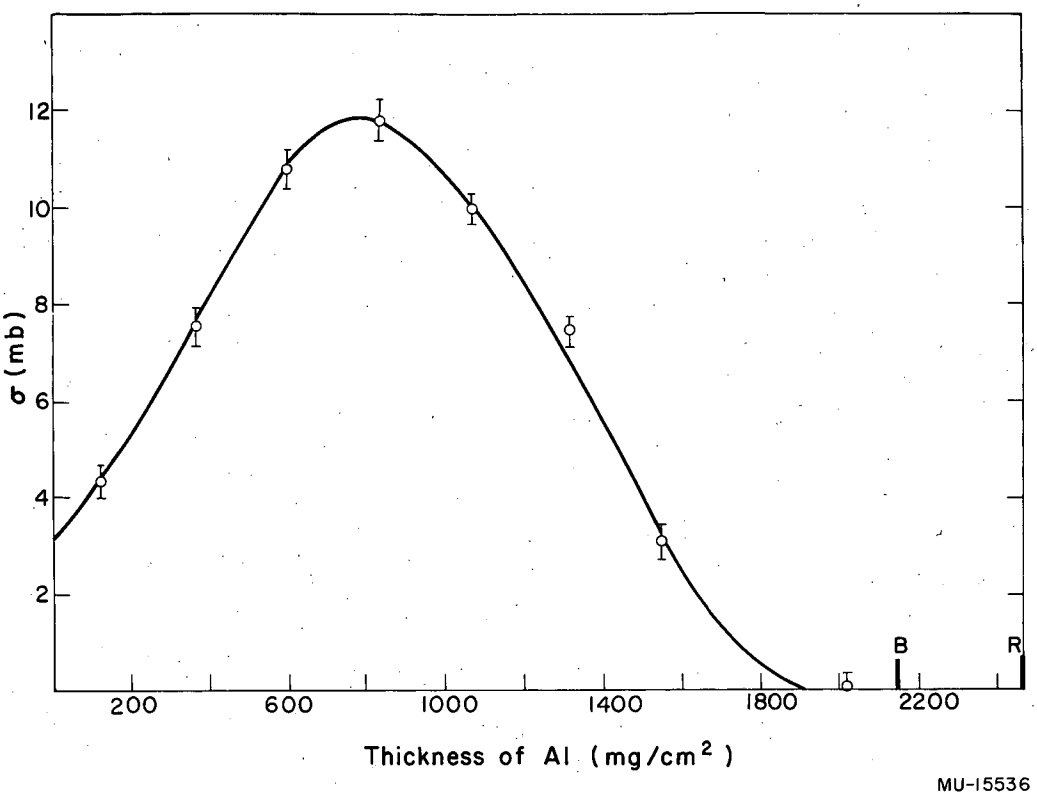

Fig. 4. Apparent excitation function for the $Au^{197}(p,t)Au^{195}$ reaction.

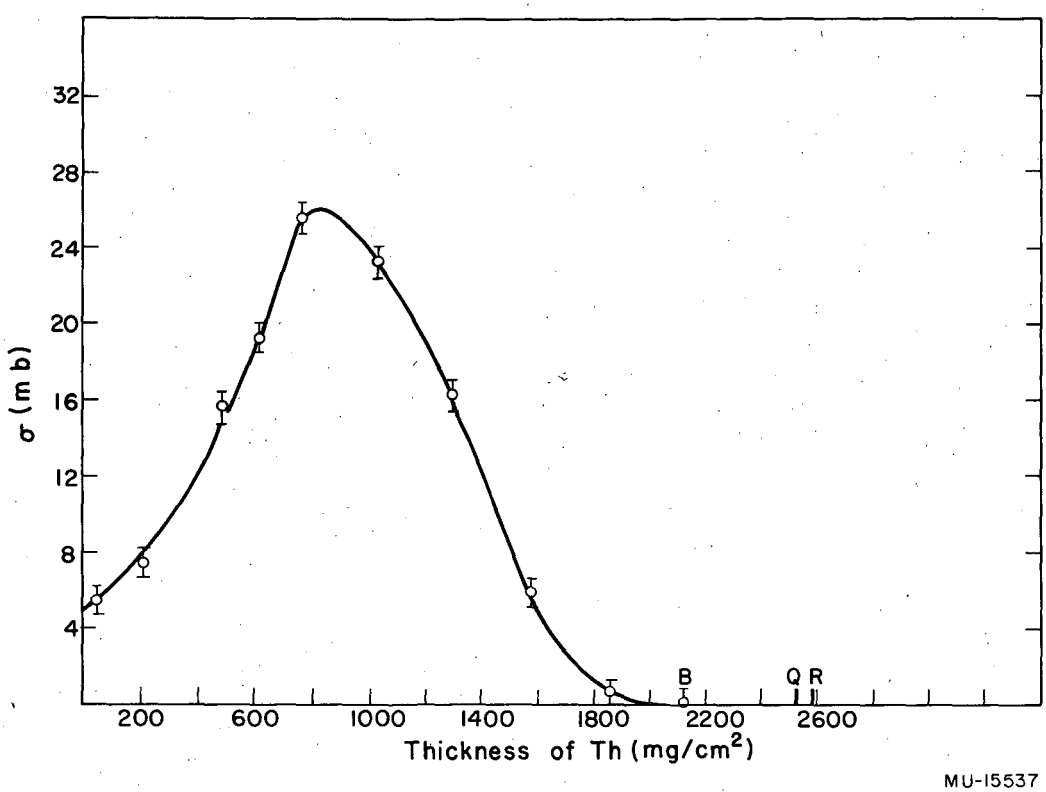

Fig. 5. Apparent excitation function for the $Th^{232}(p,t)Th^{230}$ reaction.

(d,t) cross-sections

Figures 6 to 8 represent the same type of curves for (d,t) reactions. Here, however, the tritium distribution is, in general, somewhat narrower than in the previous case. Another new feature is that in some cases tritons appear when the beam no longer has enough energy to overcome the classical potential barrier (Fig. 8) or even after the beam has too little energy to provide for the Q of the reaction (Fig. 7).

(α,t) cross-sections

The (α,t) case shows some very interesting features. From the shapes of the apparent excitation functions, the periodic table can be divided into three regions. First, there is a light-element region (Fig. 9) of which only two cases have been studied: magnesium and aluminum. Their excitation functions are characterized by a peak occurring in foils in which the beam still has high energy and a large "tail" extending well beyond the point at which the beam has been completely degraded.

Second, there is a region of medium-weight elements (Fig. 10) extending from about titanium to the neighborhood of silver. The characteristic of this region is the appearance of two peaks, a first peak similar to that of the preceding region, and a second peak which appears in foils that the beam has never reached.

Figure 11 for a heavy nonfissionable element and Fig. 12 for a heavy fissionable element represent two typical cases of the third region. Here only one peak is in evidence; it always appears at a target depth greater than the beam range.

Since the minimum in the second region appears roughly in the middle of the stack of foils, and since this place is the most likely to lose tritium by diffusion because of thermal effects, it was thought necessary to make sure that heating was not the cause of the observed doubly peaked excitation functions. This was accomplished by bombarding thin stacks which extended only to the minimum of the excitation function; if the minima were not real they should disappear under these conditions. A typical result of these experiments is shown in Fig. 10 by the points enclosed in squares. As can be seen, this evidence confirms the reality of the first peak.

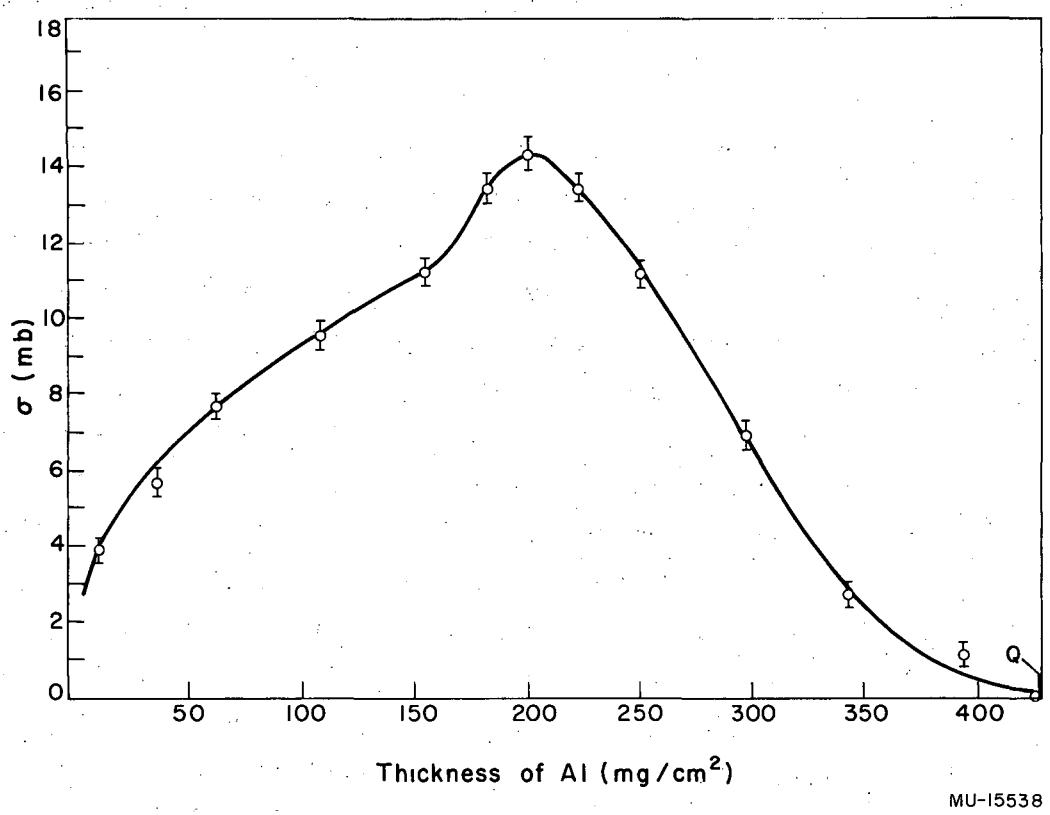

Fig. 6. Apparent excitation function for the $Al^{27}(d,t)Al^{26}$ reaction.

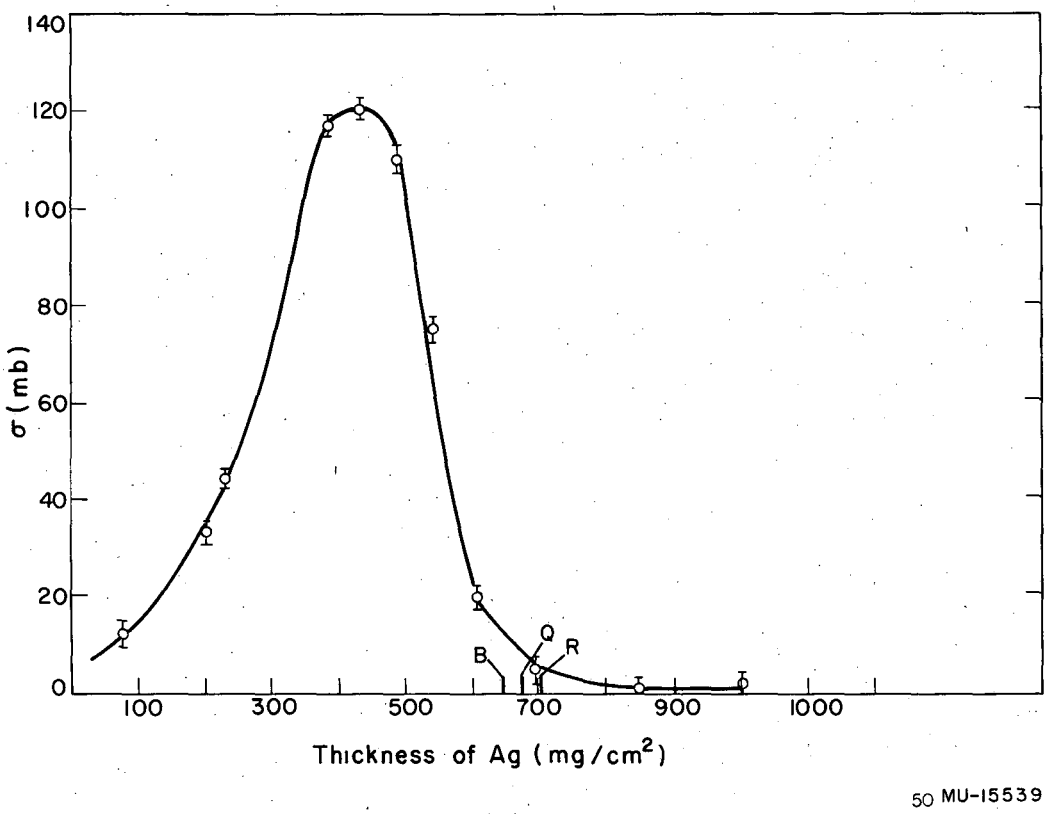

Fig. 7. Apparent excitation function for the $Ag^{107,109}(d,t)Ag^{106,109}$ reaction.

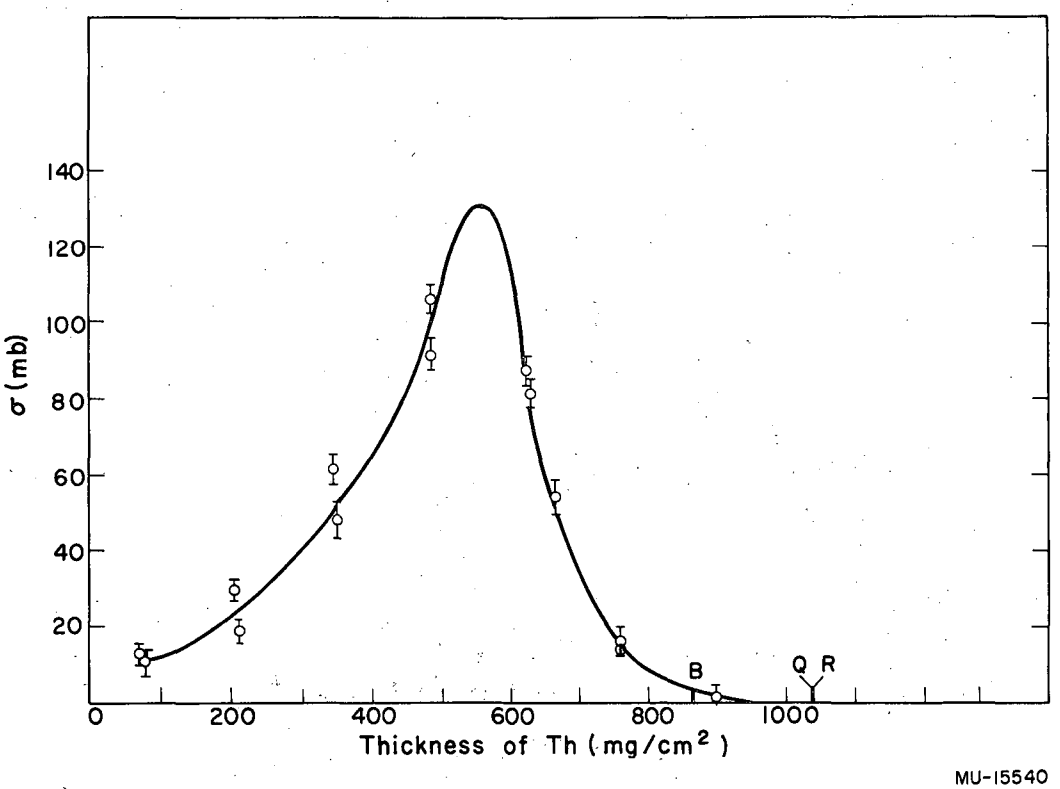

Fig. 8. Apparent excitation function for the $Th^{232}(d,t)Th^{231}$ reaction.

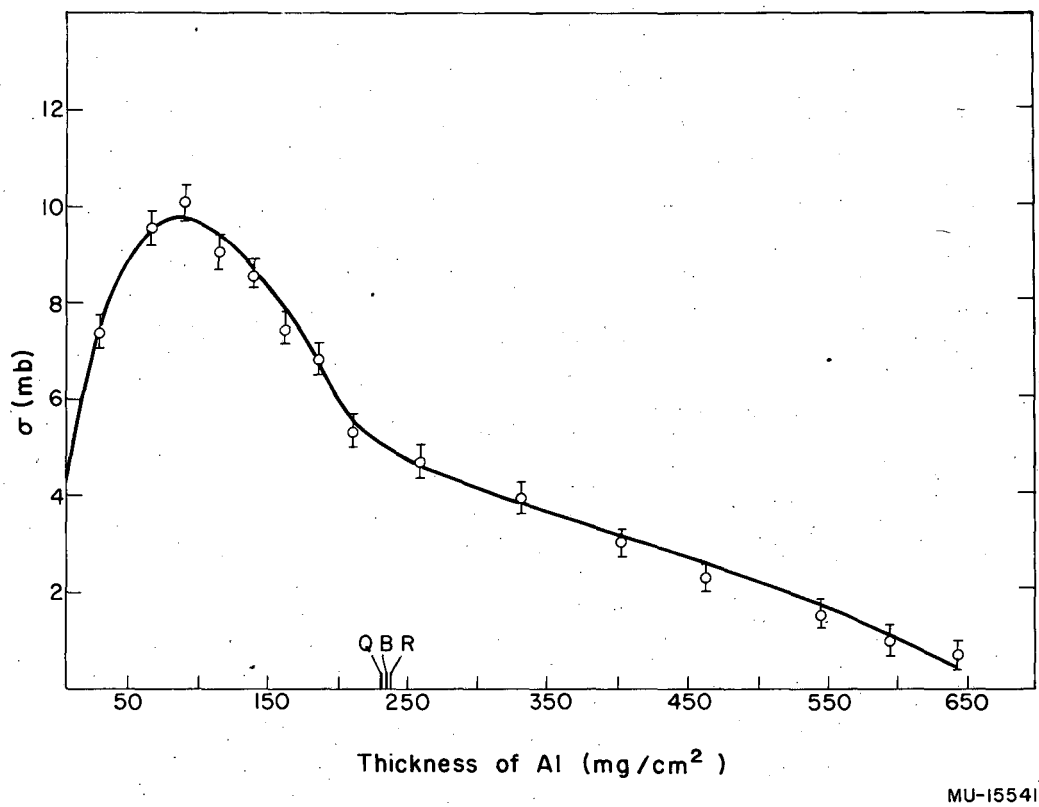

Fig. 9. Apparent excitation function for the $Al^{27}(\alpha,t)Si^{28}$ reaction.

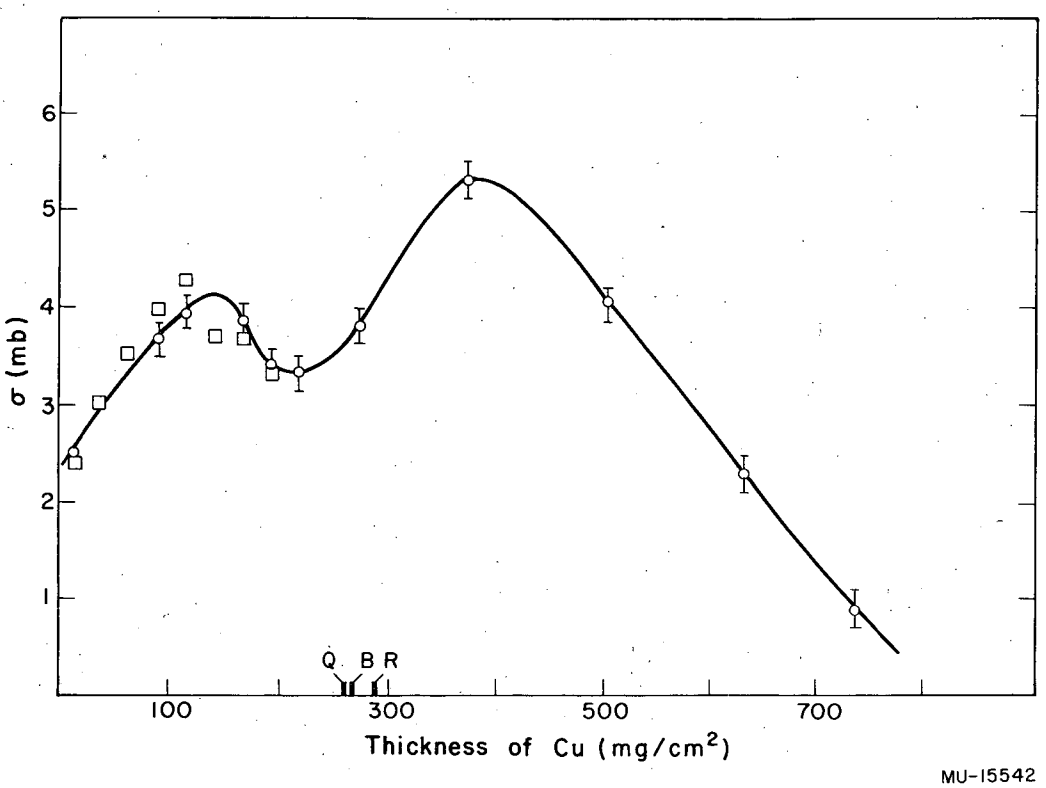

Fig. 10. Apparent excitation function for the $Cu^{63,65}(\alpha,t)Zn^{64,66}$ reaction.

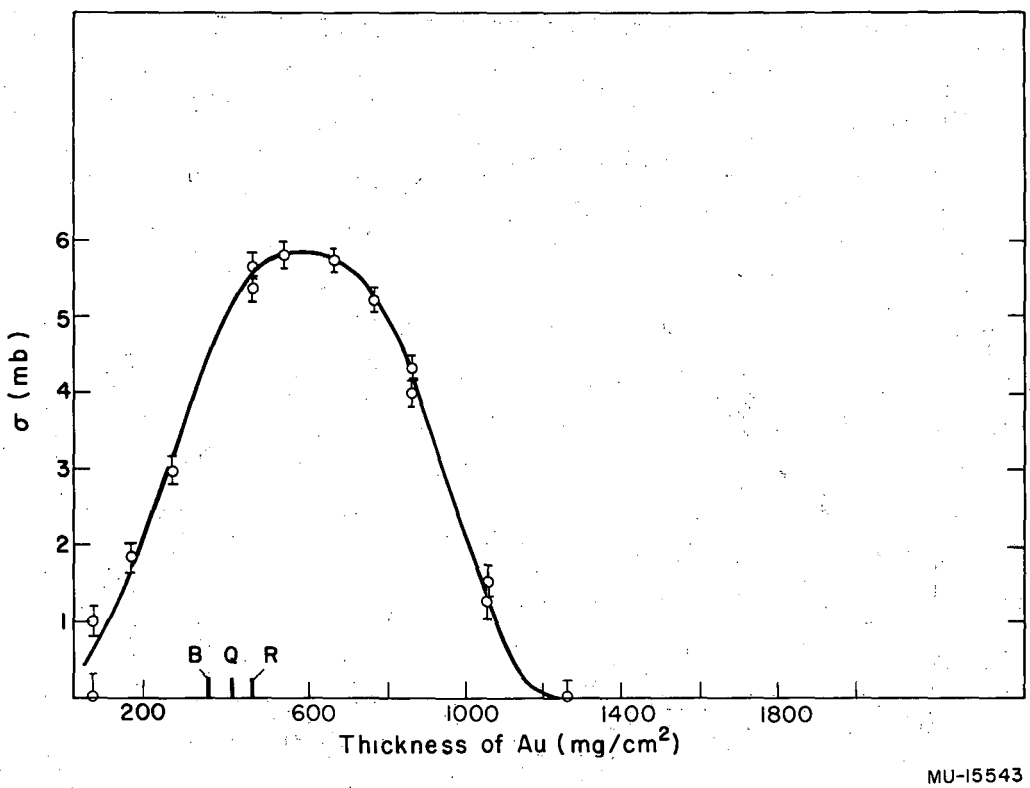

Fig. 11. Apparent excitation function for the $Au^{197}(\alpha,t)Hg^{198}$ reaction.

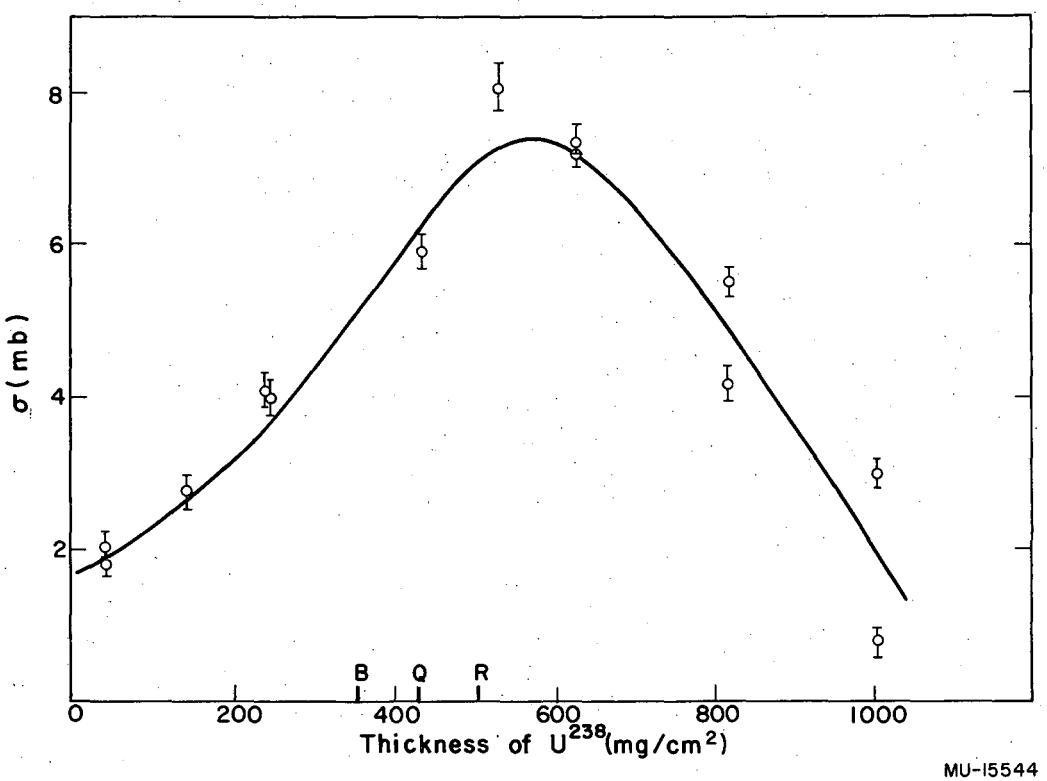

Fig. 12. Apparent excitation function for the $U^{238}(\alpha,t)Np^{239}$ reaction.

Integrated cross-sections

The integrated cross-sections ($\sum_{1}^{x(max)} \sigma_x \Delta_x$) in mb-cm for (p,t) and (d,t) reactions are shown in Tables I and II. These tables also show the yield of tritons per incident particle for these reactions. This last column of data is plotted in Figs. 13 and 14 as a function of nuclear charge. (The last two columns in Tables I and II are explained later.)

Table I

(p,t) reactions

Element	Integral (mb-cm)	Integral t/p ($\times 10^5$)	R_{eff}/R	Triton-emission probabilities ($\times 10^5$)
Al^{27}	0.589	3.55 ± .30	0.99	3.51
Cu	0.500	4.20 ± .39	0.94	3.95
Zn	0.491	3.25 ± .32	0.91	2.96
Ag	0.393	2.31 ± .21	0.92	2.13
Cd	0.654	3.04 ± .28	0.92	2.80
Au^{197}	0.685	4.03 ± .52	0.84	3.39
Pb	1.55	5.11 ± .51	0.82	4.19
Th^{232}	2.43	7.35 ± .75	0.79	5.81
U^{238}	1.37	6.50 ± .67	0.81	5.27

Table III shows the same type of data for (α,t) reactions. For this case the apparent excitation functions from the first and second regions of the periodic table can be roughly analyzed into two components: a component corresponding to low-energy tritons, which will be later identified with tritons emerging through a compound-nucleus mechanism: and a component corresponding to high-energy tritons, which will be identified with tritons produced by direct interactions. For the intermediate region the resolution of the excitation functions was carried out by assuming the second peak to have the same shape as an average peak for the heavy region. This average peak was normalized, in peak height, to the observed second peak of the intermediate region. The

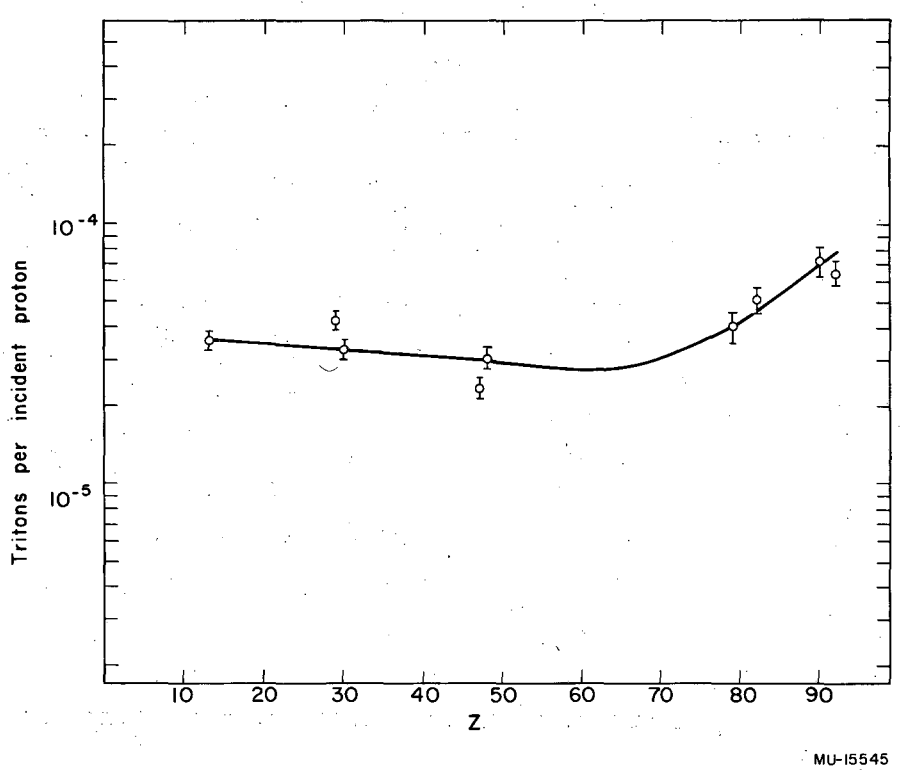

Fig. 13. Tritons per incident proton vs atomic number Z.

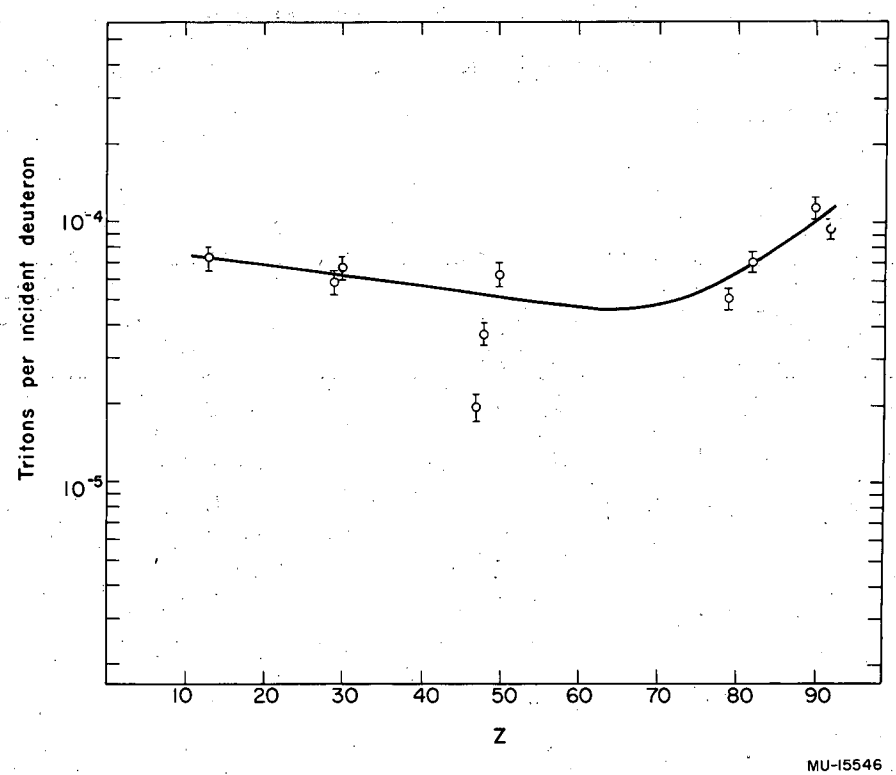

Fig. 14. Tritons per incident deuteron vs atomic number Z.

shape of the first peak of the intermediate region was then obtained by subtraction of the forward part of this normalized peak from the excitation function. For the light region the analysis was made by assuming the real shape of the peak to be symmetrical so that the high-energy component could be obtained by subtraction from the total excitation function. The total triton yields and the yields associated with each of these components are tabulated in Table III and plotted in Fig. 15 as a function of Z.

Table II

(d,t) reactions

Element	Integral		R_{eff}/R	Triton-emission probabilities ($\times 10^5$)
	(mb-cm)	t/d ($\times 10^5$)		
Al^{27}	1.20	7.23 ± .69	0.79	5.71
Cu	0.694	5.83 ± .55	0.85	4.96
Zn	0.997	6.60 ± .67	0.76	5.02
Ag	0.333	1.97 ± .25	0.87	1.71
Cd	0.785	3.65 ± .37	0.88	3.21
Sn	1.71	6.35 ± .60	0.92	5.84
Au^{197}	0.857	5.04 ± .45	0.87	4.38
Pb	2.15	7.10 ± .71	0.85	6.04
Th^{232}	3.76	11.4 ± 1.10	0.84	9.58
U^{238}	1.99	9.45 ± .75	0.84	7.94

Triton-emission probabilities

A more significant measure of triton-emission probability than the number of tritons per incident particle is given by multiplying this last quantity by the ratio of effective range to total range.

Effective range is here defined as the range at which the beam has just enough energy either to overcome the classical Coulomb barrier or to supply the reaction energy Q, whichever is higher.

Even though this correction is only approximate it helps to make comparison between different elements more meaningful.

Table III

(α,t) Reaction. Integral cross sections

Element	mb-cm	Total t/α (x10^5)	t/α (x10^{-5})		
			Radiochemical value	Compound nucleus	Direct interaction
Mg	0.767	3.35 ± .30	...	1.77	1.58
Al^{27}	1.17	7.04 ± .65	...	3.04	4.00
Ti	0.666	3.74 ± .40	...	...	...
Fe	0.269	2.28 ± .21	...	0.52	1.76
Co	0.286	2.53 ± .22	...	...	...
Ni	0.153	1.37 ± .10	...	0.29	1.08
Cu	0.305	2.56 ± .29	...	0.42	2.14
Zn	0.279	1.85 ± .17	...	...	...
Ag	0.326	1.92 ± .18	...	0.05	1.87
Cd	0.213	0.99 ± .08	...	...	0.99
In	0.423	1.65 ± .17	...	...	1.65
Sn	0.365	1.35 ± .12	...	...	1.35
Sb	0.569	1.86 ± .17	...	...	1.86
Pt	0.254	1.68 ± .15	...	...	1.68
Au^{197}	0.218	1.28 ± .11	...	...	1.28
Pb	0.339	1.12 ± .11	...	...	1.12
Th^{232}	0.515	1.56 ± .13	1.27[a]	...	1.56
U^{238}	0.260	1.23 ± .09	1.08[b]	...	1.23

[a] Assuming a counting efficiency of 100%.[1]

[b] Assuming a counting efficiency of 70%.[5]

The values of these ratios of effective range to total range (R_{eff}/R), together with the corresponding emission probabilities, are given in Tables I, II, and IV and Figs. 16 to 18 for (p,t), (d,t), and (α,t) reactions respectively. It can be seen that this correction does not significantly change the shape of the triton-yield functions.

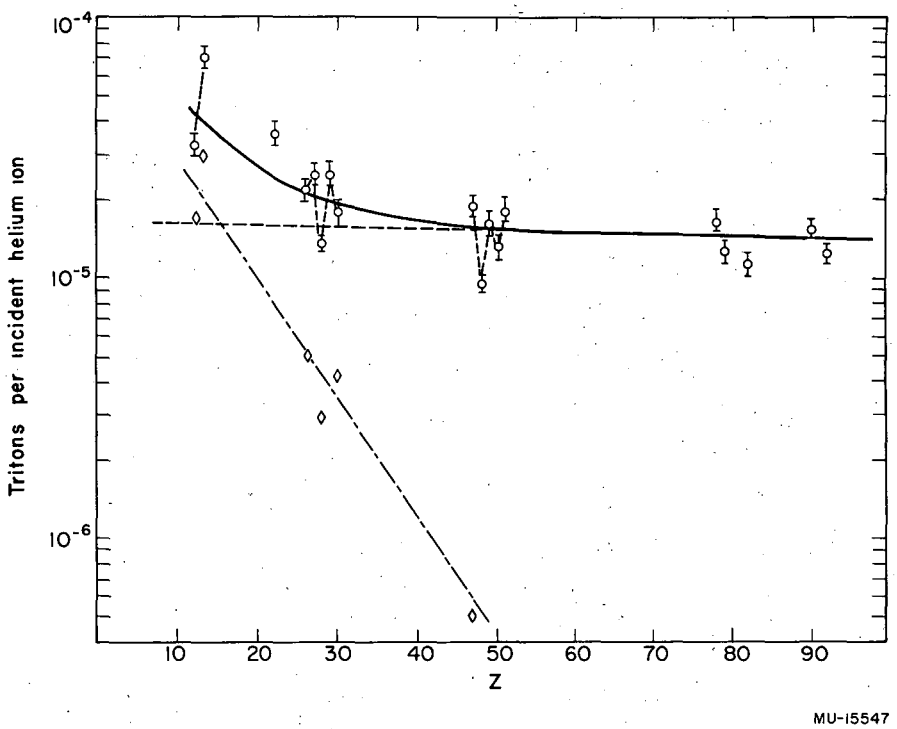

Fig. 15. Tritons per incident helium ion vs atomic number Z.
⊙ ——— total number of tritons per incident helium ion.
– – – – direct-interaction contribution.
◇ —.—.— compound-nucleus contribution.

Table IV

(α,t) reaction. Tritium-emission probabilities

Element	R_{eff}/R	Total probability ($\times 10^5$)	Compound-nucleus contribution ($\times 10^5$)	Direct-interaction contribution ($\times 10^5$)
Mg	0.92	3.08	1.63	1.45
Al^{27}	0.96	6.76	2.92	3.84
Ti	0.89	3.33	...	...
Fe	0.88	2.01	0.47	1.54
Co	0.92	2.33	...	...
Ni	0.93	1.27	0.27	1.01
Cu	0.90	2.30	0.38	1.92
Zn	0.85	1.57	...	...
Ag	0.87	1.67	0.04	1.63
Cd	0.86	0.85	...	0.85
In	0.87	1.44	...	1.44
Sn	0.86	1.16	...	1.16
Sb	0.85	1.58	...	1.58
Pt	0.76	1.28	...	1.28
Au^{197}	0.75	0.96	...	0.96
Pb	0.73	0.82	...	0.82
Th^{232}	0.72	1.12	...	1.12
U^{238}	0.70	0.86	...	0.86

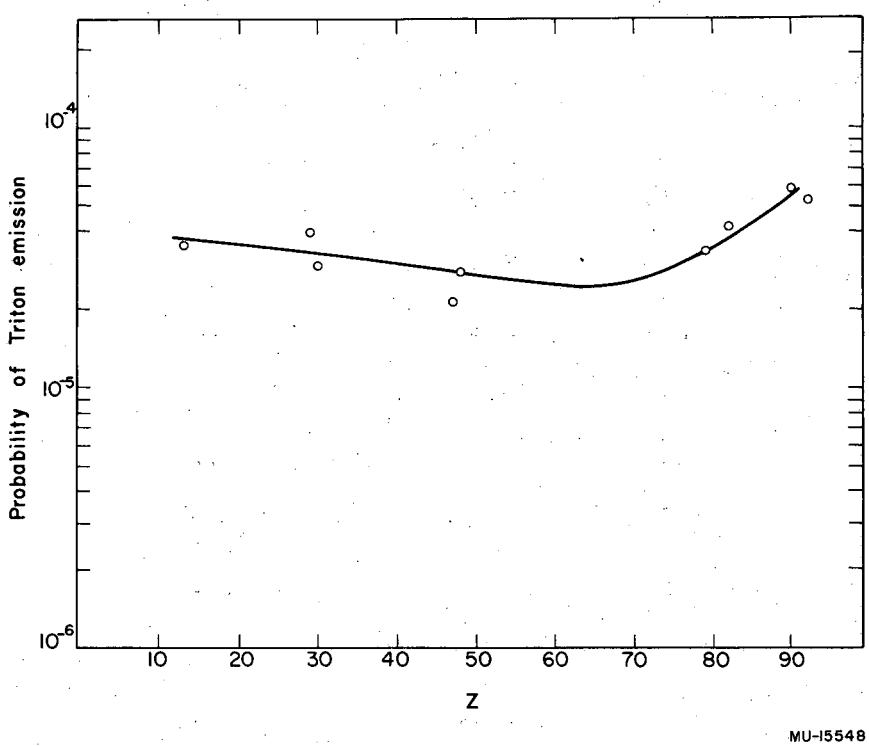

Fig. 16. Probability of triton emission in the (α,t) reaction vs atomic number Z.

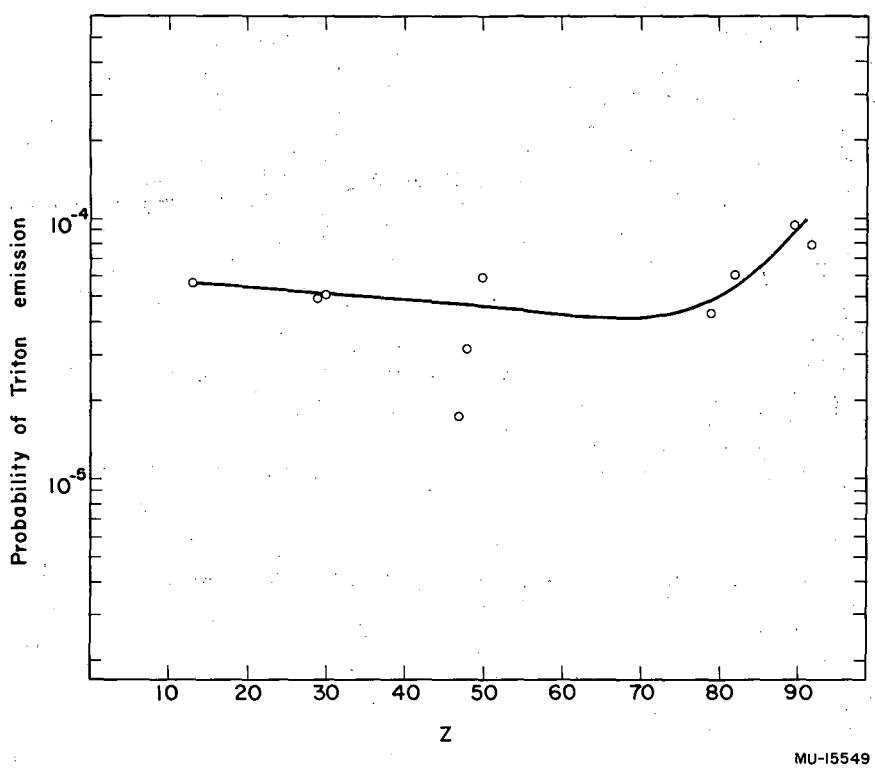

Fig. 17. Probability of triton emission vs atomic number for the (d,t) reaction.

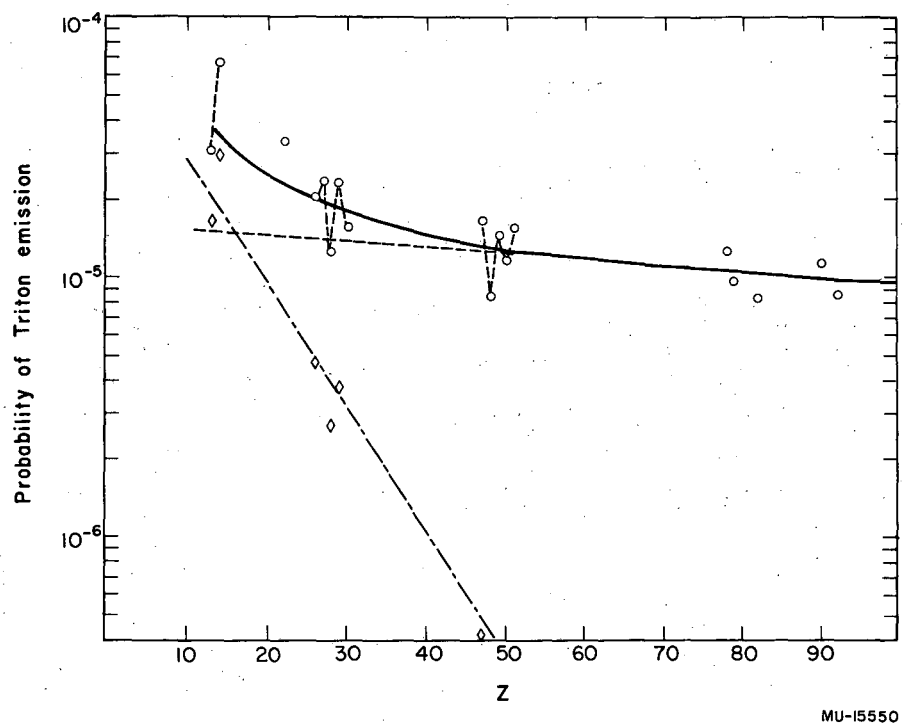

Fig. 18. Probability of triton emission vs atomic number in the (α,t) reaction.

total probability of triton emission for this reaction.
compound-nucleus contribution
direct-interaction contribution.

B. Angular Distributions

$Al^{27}(\alpha,t)Si^{28}$

Figure 19 shows the spectrum of tritons arising from the $Al^{27}(\alpha,t)Si^{28}$ reaction leading to the ground state and first excited state of Si^{28} at a laboratory-system angle of 7.5°. The ratio of peak height to background is 2:1 for the ground-state peak and 1.2:1 for the first-excited-state peak. The triton ranges are in good agreement with theoretical calculations based on reaction energetics.

Figure 20 shows the same spectrum at 55° (lab). The ratios of peak height to background have dropped to 1.1:1 and 1.1:1 for the peaks corresponding to the ground state and first excited state respectively. This illustrates part of the experimental difficulties of the procedure. The range resolution was about 3%, corresponding to an energy resolution of 1.7%.

Table V shows the variation of differential cross-section with center-of-mass angle for this reaction. Figures 21 and 22 show a plot of these data together with theoretical curves calculated in accordance with Butler's theory.

Determination of $d\sigma/d\Omega$ at 154° shows that the differential cross-section is ~0 at large angles.

Integration of the differential cross-sections was carried out in accordance with the well-known equation

$$\sigma = 2\pi \int d\sigma/d\Omega \sin\theta \, d\theta ,$$

which yielded a cross section of 262 mb for the transition corresponding to the ground state of Si^{28} and 101 mb for the first excited state, giving a total cross-section of 363 mb. The equivalent yields of these cross-sections are respectively 9.76×10^{-6}, 3.76×10^{-6}, and 1.35×10^{-5} tritons per incident helium ion.

$Fe^{56}(\alpha,t)Co^{57}$

The spectrum of tritons arising from this reaction at 15° (lab) is shown in Fig. 23. The assignment of the peaks is indicated in the

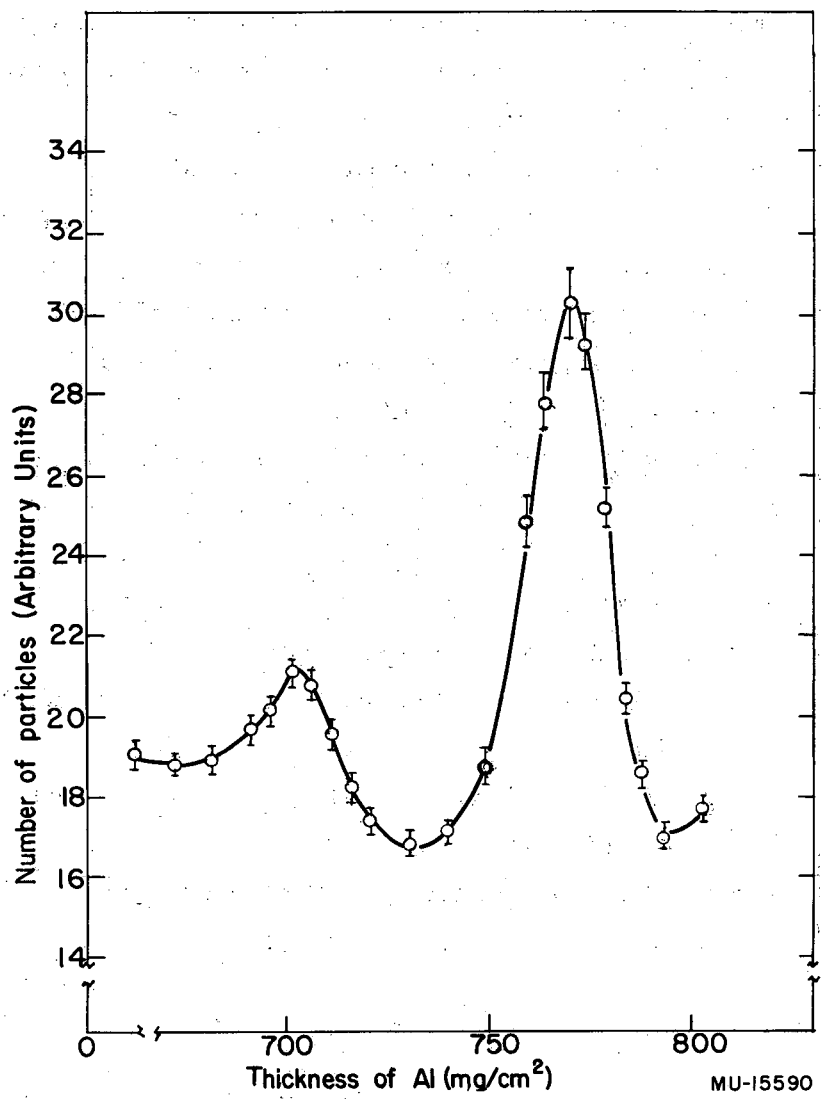

Fig. 19. Spectrum of tritons corresponding to the ground state and first excited state of Si^{28}, from the reaction $Al^{27}(\alpha,t)Si^{28}$ at $\theta_{\ell} = 7.5^{\circ}$.

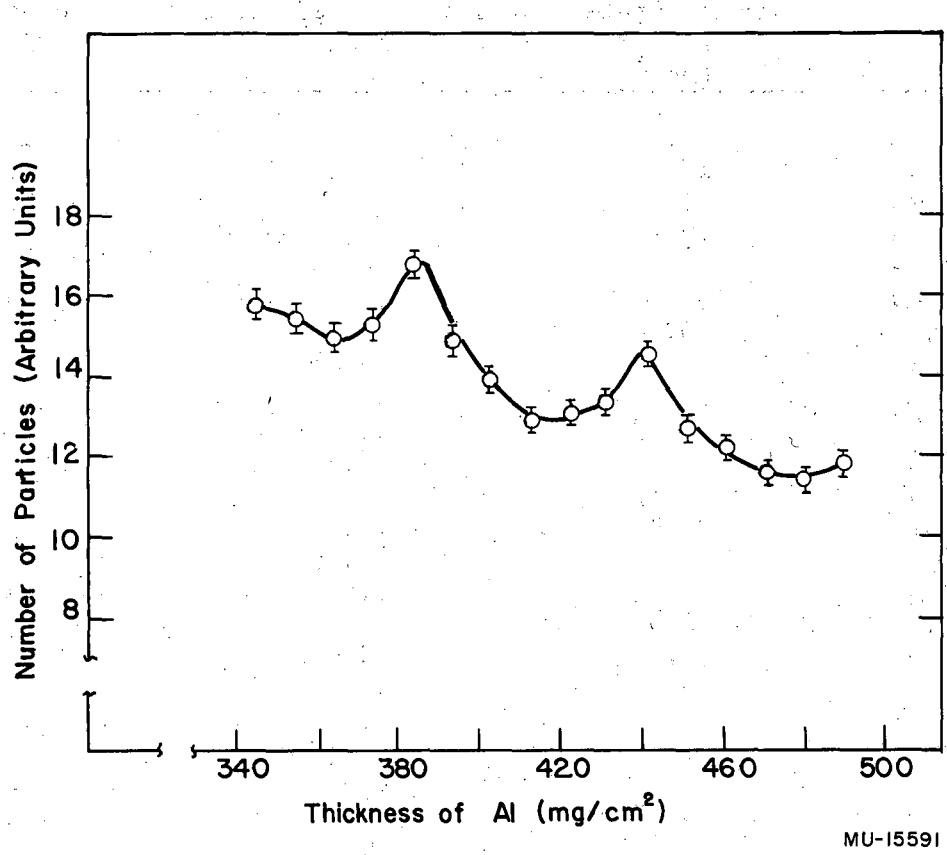

Fig. 20. Spectrum of tritons corresponding to the ground state and first excited state of Si^{28}, from the reaction $Al^{27}(\alpha,t)Si^{28}$ at $\theta_{\ell} = 55^{\circ}$.

Table V

Differential cross sections as a function of center-of-mass angle

	$Al^{27}(\alpha,t)Si^{28}$		$Fe^{56}(\alpha,t)Co^{57}$
θ c.m.	$d\sigma/d\Omega$ of tritons leading to ground state of Si^{28} (mb)	$d\sigma/d\Omega$ of tritons leading to first excited state of Si^{28} (mb)	$d\sigma/d\Omega$ of triton leading to ground state of Co^{57} (mb)
7.51	...	...	11.6
8.00	18.42	3.91	...
10.75	...	...	10.1
11.39	13.39	...	...
11.44	...	4.64	...
13.40	...	...	4.88
13.73	9.52	...	...
14.30	...	3.68	...
16.11	...	...	2.74
17.08	3 95	...	...
17.15	...	1.91	...
21.47	...	...	1.49
22.74	2.46	...	...
22.84	...	0.95	...
26.82	...	...	1.10
28.39	1.60	...	...
28.51	...	0.88	...
32.15	...	...	0.59
34.01	1.55	...	...
34.16	...	0.68	...
37.47	...	...	0.61
39.61	0.85	...	...
39.77	...	0.39	...
45.16	0.59	...	...
45.35	...	0.39	...
48.04	...	...	0.25
50.68	0.59	...	...
50.88	...	0.34	...
61.59	0.28	...	...
61.82	...	0.24	...

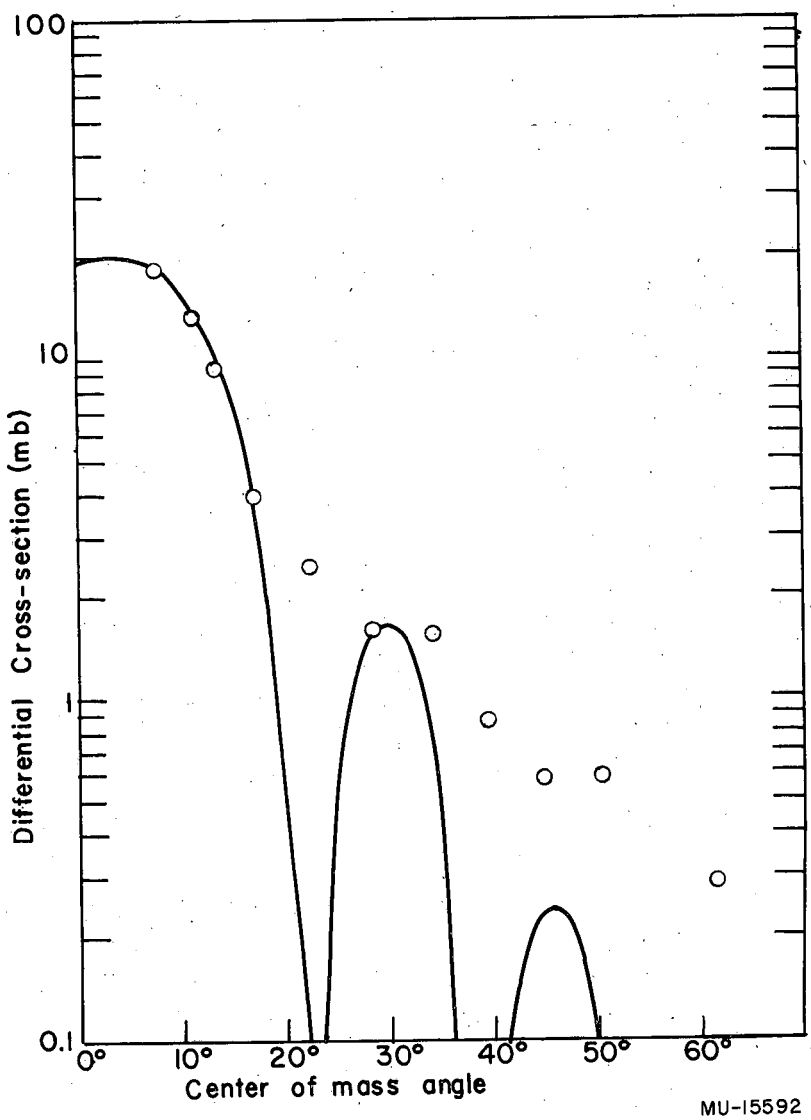

Fig. 21. Angular distribution of tritons from the $Al^{27}(\alpha,t)Si^{28}$ reaction leading to the ground state of Si^{28}. The encircled points represent the experimental data. The solid line is a theoretical curve calculated according to Butler's theory with $r = 5.85 \times 10^{-13}$ cm and $\ell = 3$.

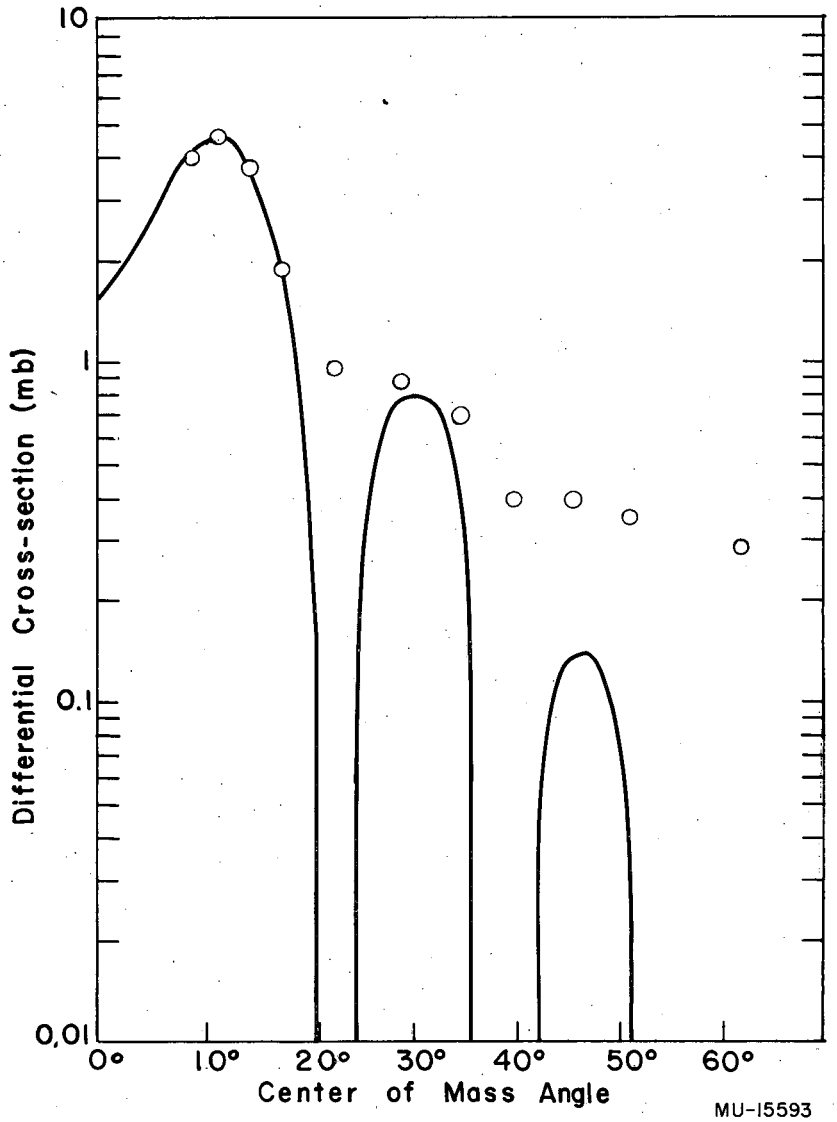

Fig. 22. Angular distribution of tritons from the $Al^{27}(\alpha,t)Si^{28}$ reaction leading to the first excited state of Si^{28}. The encircled points represent the experimental data. The solid line is a theoretical curve calculated according to Butler's theory with $r = 5.65 \times 10^{-13}$ cm and $\ell = 0$.

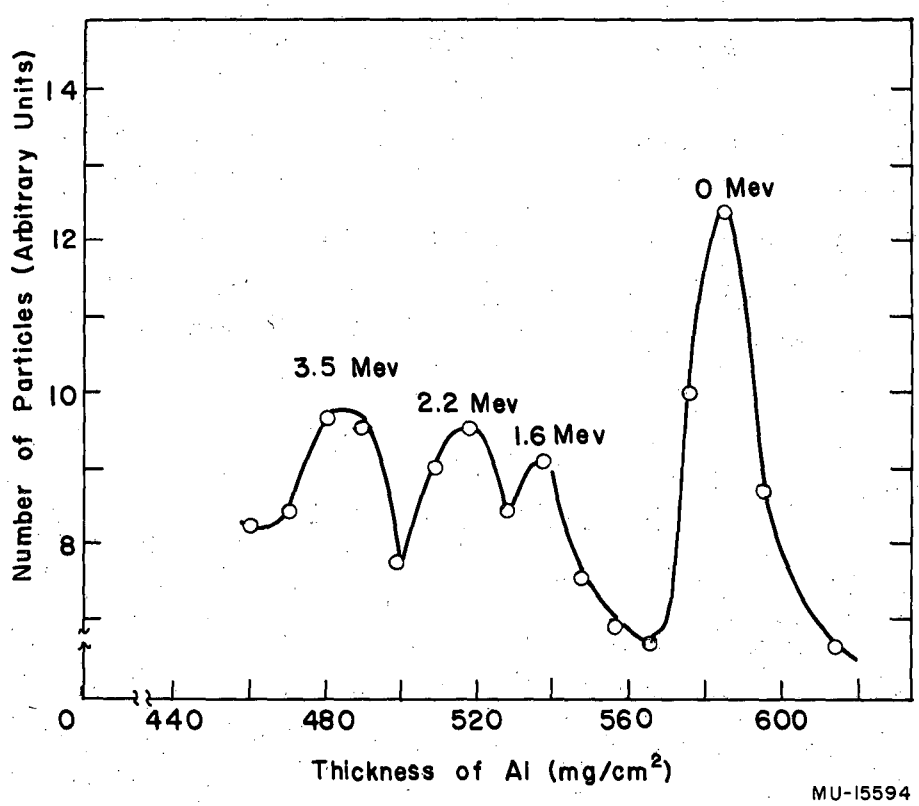

Fig. 23. Triton spectrum from the $Fe^{56}(\alpha,t)Co^{57}$ reaction at $\theta_\ell = 15^\circ$. The energies indicated in the graph are measured with respect to the ground-state peak.

figure. The three small peaks on the left of the large peak corresponding to the ground state of Co^{57} agree roughly with the known level of Co^{57}. The position of the ground-state peak was found to be in rather good agreement with that predicted from energetics. Owing to poor resolution and to background problems, only the ground-state peak was measured as a function of angle.

Figures 24 and 25 show the ground-state peak at 7° and 45° (lab) respectively.

The variation of differential cross-section with center-of-mass angle is shown in Table V. The $d\Omega/d\sigma$ is plotted in Fig. 26 together with a Butler curve corresponding to this reaction.

Integration up to 50° (c.m.) gave a total cross-section of 148 mb, corresponding to a yield of 6.41×10^{-6} tritons per incident helium ion.

DISCUSSION

Apparent Excitation Functions

(α,t) reactions

The most striking result seen upon examination of the apparent cross-sections for tritium production as a function of target depth in the (α,t) reaction is that most of the triton yield is found in foils that the beam does not reach. This observation can have only one interpretation: tritons must be emitted in the forward direction with velocities comparable to those of the helium ions. The lower degradation rate of the tritons permits them to travel farther than the helium ions and hence to be deposited in foils that the latter cannot reach. An analysis of Figs. 9 to 12 shows that the majority of the tritons must have energies between 20 and 30 Mev and be produced within a cone of total included angle of 60°.

The fact remains, however, that -- in some regions of the periodic table at least -- there is an appreciable contribution of low-energy tritons. The peak observed in the light-element region bears this type of interpretation, since the peak occurs quite early in the

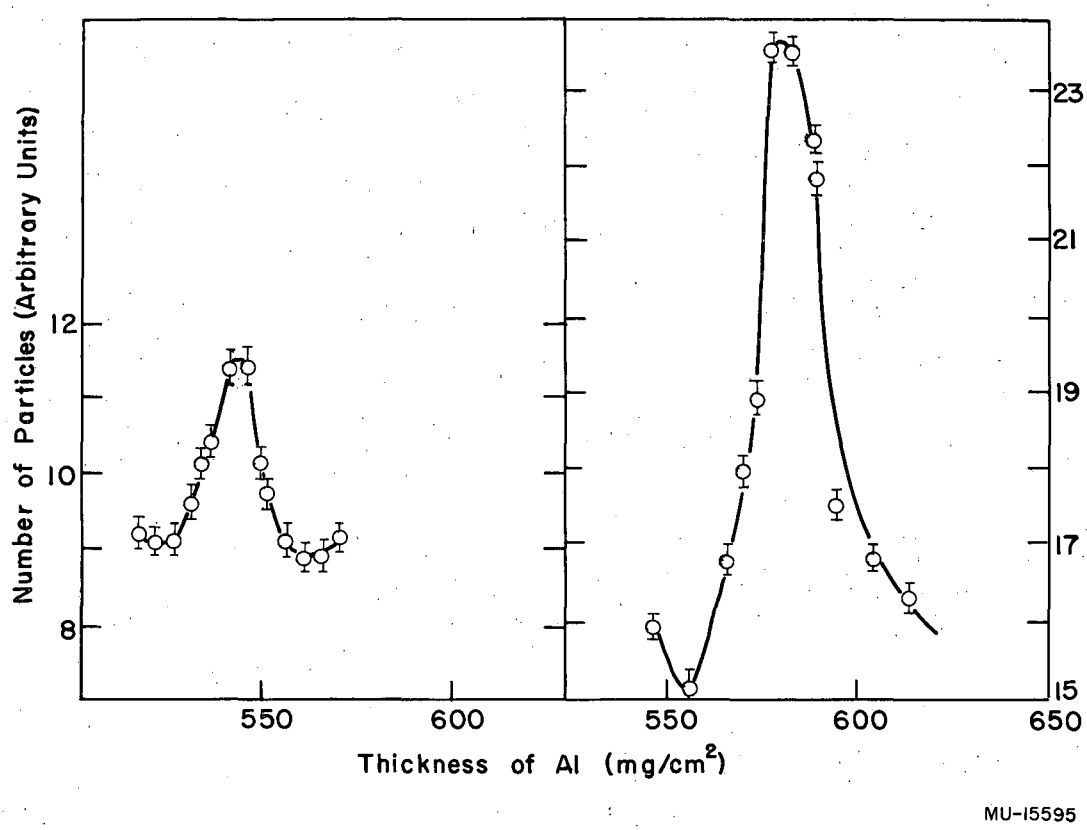

Fig. 25

Fig. 24

Fig. 24. Triton spectrum corresponding to the ground state of Co^{57} from the $Fe^{56}(\alpha,t)Co^{57}$ reaction, at $\theta_\ell = 7^\circ$.

Fig. 25. Triton spectrum corresponding to the ground state of Co^{57} from the $Fe^{56}(\alpha,t)Co^{57}$ reaction, at $\theta_\ell = 45^\circ$.

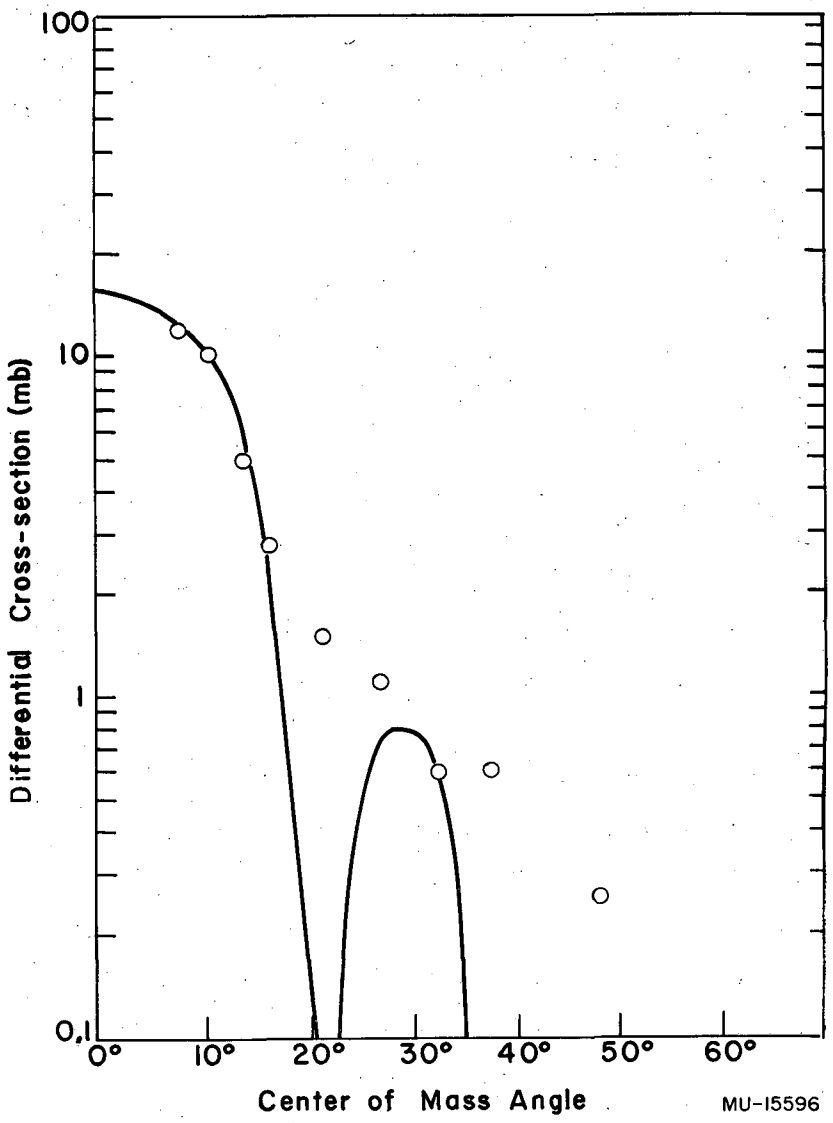

Fig. 26. Angular distribution of tritons from the $Fe^{56}(\alpha,t)Co^{57}$ reaction leading to the ground state of Co^{57}. The encircled points represent the experimental data. The solid line is a theoretical curve calculated according to Butler's theory with $r = 5.85 \times 10^{-13}$ cm and $\ell = 3$.

foil stack, showing that the tritons stopping in this region did not have long ranges and hence must have had small energies. The most likely mechanism for the production of low-energy tritons is a compound-nucleus process. Such a mechanism should produce charged particles with energies in the neighborhood of their classical Coulomb barriers. A simple calculation shows that the peak occurs at a distance from the beginning of the foil stack that is roughly equivalent to the range of a triton with an energy equal to the Coulomb barrier, indicating that most of the compound-nucleus tritons are produced in the first few foils. Even though compound-nucleus tritons should be emitted roughly isotropically in the center-of-mass system, the velocity of the center of mass in the laboratory system is such that the tritons tend to move, in general, in a forward direction. The loss of low-energy tritons due to backward motion can be estimated in the neighborhood of 15% of the compound-nucleus contribution. Of course, as the beam gets degraded the forward component of velocity becomes smaller, but by then the range that the tritons have to travel to get out of the stack has increased, so that the losses are minimized. This last effect also tends to accumulate low-energy tritons at the beginning of the stack. The foregoing also applies to the first peak of the intermediate region.

The second peak of the intermediate region and the peak of the heavy-element region, both of which occur after the beam has been completely degraded, must be produced by high-energy tritons and indicate a predominant direct-interaction mechanism for the reaction.

(p,t) and (d,t) reactions

The interpretation of the apparent excitation functions for (p,t) and (d,t) reactions is not as clear-cut as for the (α,t) reaction, because of the longer range of protons and deuterons in comparison with the helium ions.

All the (p,t) cross section occurs in foils in which the beam has enough energy left both to overcome the classical Coulomb barrier and to furnish the Q of the reaction.

In the (d,t) reaction there is, however, some evidence for high-energy tritons. For most cases (See Figs. 7 and 8) tritons are observed in foils in which the beam cannot overcome the Coulomb barrier, and in some cases (see Fig. 7) tritons are observed in regions beyond those in which the beam has enough energy to produce the reaction.

Integrated Cross Sections and Triton Yields

(p,t) reactions

Not many workers have studied (p,t) reactions in great detail. However, there seems to be good, if fragmentary, evidence that at low Z the compound-nucleus mechanism plays a very important role in the production of tritium from proton bombardments. Cohen and Handley studied (p,t) reactions in a few light elements (beryllium, iron, niobium, and palladium), using proton energies ranging from 14 to 22 Mev.[15] They concluded that direct-interaction processes, i.e., double pickup of two neutrons by the proton, were important only when the target element has two neutrons outside a closed shell, and that calculations[31] of the inherent probability of triton emission from their data and compound-nucleus considerations show this probability to be not much (if any) less than for the emission of protons and neutrons. This last result is rather startling, because even though the implicit assumption in the compound-nucleus model is that aside from Coulomb barrier effects all particles are emitted with equal probability, a greater inherent probability would be expected for the emission of a neutron or a proton than for a complex and loosely bound structure such as a triton,[32,33]

Currie, Libby, and Wolfgang[14] studied (p,t) reactions at much higher energies (450 and 2040 Mev) for a series of elements ranging from aluminum to lead. They found again that the compound nucleus plays a significant role in the mechanism. They were successful in showing that the experimental triton multiplicities at 450 Mev follow roughly the theoretical compound-nucleus multiplicities[34] from

aluminum to iron but not beyond; at 2040 Mev the disagreement starts earlier in Z. Beyond this last point of agreement the cross section increases again, suggesting the taking over by a different mechanism.

Figure 16 shows the results of this work for (p,t) reactions. The cross sections are expressed as triton-emission probabilities and are plotted against Z of the target material. The curve exhibits a behavior similar to that described by Currie et al. at much higher energies.[14] The shape of the curve could, then, be interpreted as follows: the reaction proceeds by two contributing mechanisms, compound-nucleus processes and direct interactions. Owing to Coulomb-barrier effects[35] the compound-nucleus processes can be expected to be relatively more important at low Z and to decrease in importance as Z increases. Then the relative importance of the direct-interaction processes increases and finally takes over. Direct interactions are considered to take place mostly on the rim of the nucleus.[36-39] Then the cross-section for direct interactions could be expected to increase roughly as the nuclear circumference if it were not for the fact that the increasing nuclear charge limits the number of partial waves that are able to take part in the reaction; however, a simple approximate calculation based on Rutherford's scattering equation shows that the cross section actually increases as the nuclear radius increases in spite of the Coulomb effect. Then the expected shape of the integrated cross-section curve as a function of Z would be a decrease collowed by a leveling off and finally an increase of the cross-section values. Such is the behavior observed. The fact that the turnover of the probability curve occurs at a Z of about 60 to 70 seems to be in line with the trend shown in the work by Currie et al.[14]

Kundu and Pool[40] were able to explain satisfactorily the behavior of (t,p) reactions by a double neutron stripping of the triton. On the basis of the principle of detailed balance of nuclear reactions,[35] it would therefore be expected that double pickup of two neutrons by a proton is an important component of the direct-interaction mechanism. If this is true the neutron-to-proton ratio should

be another important factor in determining the shape of the curve representing the triton-emission probability vs Z, since a greater abundance of neutrons on the nuclear surface should tend to make the pickup process more probable. However, knock-on reactions cannot be excluded, at least in the low-atomic-weight region, if the evidence for preformed complex units in the nucleus given by Cohen and Handley[15] is to be believed.

(d,t) reactions

Deuteron-induced reactions have been the subject of extended theoretical treatments by Peaslee,[41] Newns,[42] Butler,[36] and others. Deuteron-induced reactions in the light-element region have also been subjected to intensive experimental investigation.[43-49] Consequently it is not surprising that (d,t) reactions have been the object of more extensive studies[50-52] than the (p,t) reactions. The evidence of these studies seems to indicate that for low Z and low bombarding energy (< 3 Mev) the bulk of the (d,t) reaction can be accounted for by compound-nucleus processes. However, at higher energies the work of Vogelsang and McGruer[50] shows that at a bombarding energy of 14.8 Mev direct interaction processes are very important for Na^{23}, and that the triton angular distributions of the reaction can be accounted for by Butler's treatment. Wolfgang and Libby have demonstrated that in beryllium up to 7.7 Mev the probability for the (d,t) reaction is comparable with the probabilities for (d,p) and (d,α) reactions, and as large as that for (d,n) reactions.[22] Harvey studied (d,t) reactions in Au^{197} and found the direct-interaction process to be quite prevalent.[19] Butler[36] and Newns[42] consider that (d,t) reactions, when proceeding by direct interaction, do so by a pickup mechanism.

It could be expected, then, since the same factors involving the compound nucleus and direct-interaction processes are present in the (d,t) and (p,t) reactions, that the shape of the probability curves should closely resemble one another. Such is the case. This similarity in shape points towards similarly shaped true excitation functions. Furthermore,

since a single pickup should be easier to accomplish than a double pickup, the cross-section for (d,t) reactions should be greater than the cross-section for (p,t) reactions. Again, such is the case.

(α,t) reactions

From the evidence given previously (in the section dealing with the apparent excitation functions for (α,t) reactions) it is known that at low Z the compound-nucleus processes seem to play an important part in contributing to the total (α,t) cross section.

The probabilities for tritium emission in the (α,t) reaction as a function of Z are plotted in Fig. 18, which also breaks the data into compound- and non-compound-nucleus contributions. The compound-nucleus part can be seen to decrease rapidly with Z, as expected from compound-nucleus theory.[35] The non-compound-nucleus part seems to remain roughly constant throughout the periodic table, showing, perhaps, a slight decreasing trend. The fact that no final rise in the integrated cross-section curve is shown as for (p,t) and (d,t) reactions is not surprising, since in all probability the shapes of the true excitation functions are quite different.

In several regions (magnesium to aluminum, iron to zinc, and silver to antimony) of the (α,t) probability curve, where it was possible to obtain metal foils of consecutive Z, odd-even Z effects were noticed. The cross-sections for the odd-Z isotopes are, in general, higher than for the even-Z ones. This phenomenon may be connected with the extra pairing energy in the capture of a proton by an odd-Z nucleus. The fact that no magic-number effects were observed over the even-odd effects is not unusual, since it is well known that in some cases the even-odd effects are more noticeable than the former.[53] Neutron even-odd effects should also be present, but it was not possible to obtain separate isotopes in sufficient quantities to test this effect.

Additional evidence for the direct-interaction process can be obtained by the comparison of the data presented in this work with radiochemical data taken in the fissionable region for the (α,p2n) reaction,[1,5]

as shown in Table III. It appears that cross-sections determined by both methods agree with each other within 20%. Since radiochemical methods measure only those nuclei that survive fission, it would seem that for a large share of interactions the residual heavy product must be left in the ground state or in a low-lying excited state, hence able to undergo little fission competition, whereas the triton escapes with a large amount of energy. Thus it appears that most, if not all, of the $(\alpha,p2n)$ reaction in the heavy elements can be identified with an (α,t) reaction. (This part of the work presented here has appeared in an earlier publication.[54]) The fact that the integrated cross sections for tritium production are somewhat higher than the corresponding $(\alpha,p2n)$ or (α,t) cross-sections determined radiochemically may indicate the presence of a spectrum of triton energies of which approximately 20% results in residual nuclei left in states sufficiently excited to undergo fission. The differences as they stand, however, are such that it is possible that the two types of cross-sections are actually equal. It should be noted that although it is believed that the tritium activity collected and the corresponding heavy fragments observed radiochemically represent, in the main, simply (α,t) reactions, the tritium may actually result from (α,t), (α,tn), and (α,tf) reactions, and the "$(\alpha,p2n)$" products may result from (α,t), $(\alpha,p2n)$, and (α,dn) reactions.

The direct-interaction processes seem to be possible for the (α,t) reaction. One is a knock-on reaction, the other a stripping process. In the heavy elements (α,t) cross-sections are larger than (α,p) cross sections.[1-3] The (α,p) reaction is usually thought of as a knock-on reaction,[1,2,55] in which case if the (α,t) is also a knock-on reaction its cross-section ought to be smaller than the (α,p) cross-section, since the configuration X + p for the target nucleus should be more probable than a Y + t configuration. Therefore it would seem that the direct-interaction component of the (α,t) reaction is mainly the stripping of one proton from the helium ion.

Angular Distributions of the (α,t) Reaction

Butler's theory

The study of the angular distribution of products from nuclear reactions is a very powerful instrument for determining the mechanism of the reaction under consideration[35] and the angular momentum changes involved.[56,57] The advent of Butler's theory[36,58-60] was a definite step towards the interpretation of the angular distribution of direct-interaction processes.

Butler's theory was developed mainly as a means for using nuclear reactions as a tool in nuclear spectroscopy.[36,61-64] It was originally intended to cover only deuteron stripping reactions, but it was soon extended into other direct-interaction processes.[65,66]

There are two main forms of the theory, that developed by Butler,[36,58] and the one originated by Bathia, Huang, Huby, and Newns[67] which starts with the Born approximation. Both forms were proved equivalent by Daitch and French,[68] since certain of the approximations made by Butler are roughly equivalent to a Born approximation.

In its simplest form the result of Butler's theory can be written, for a given energy of incident and emitted particle,

$$d\sigma/d\Omega = A|F|^2 |j_{\ell+1/2}(\vec{q}\,\vec{r})|^2 ,$$

where $d\sigma/d\Omega$ is the differential cross-section per unit solid angle: A is a constant for a given reaction energy (it involves level widths, factors of the wave functions involved, and assorted constants); F is a form factor; $j_{\ell+1/2}(\vec{q}\,\vec{r})$ is a spherical Bessel function of order $\ell + 1/2$, where ℓ is the relative change in angular momentum between the initial and final nuclei involved; $\vec{q}$ is the vector difference between the vector wave numbers of the bombarding particle ($\vec{k}_i$) and the final light product of the reaction ($\vec{k}_f$); r is the radius of interaction, and A and $\vec{r}$ are usually taken as adjustable parameters.

The value of ℓ is determined by the usual equation for conservation of angular momentum,

$$\vec{I}_o + \vec{s}_o + \vec{\ell}_o = \vec{I}_f + \vec{s}_f + \vec{\ell}_f$$

$$\vec{\ell} = \vec{\ell}_f - \vec{\ell}_o = \vec{I}_o - \vec{I}_f + \vec{s}_o$$

$$|\vec{I}_o + \vec{I}_f + \vec{s}_o| \leq \ell \leq I_o + I_f + s_o ,$$

where $\vec{I}_o$ and $\vec{I}_f$ are the initia and final spins of the target nucleus, $\vec{s}_o$ is the intrinsic spin of the captured particle, $\vec{s}_f$ has been set equal to zero because the reaction is only with the captured particle. When several ℓ's are possible, as is usually the case, the lowest value of ℓ is taken as the one that contributes the most. In the choice of ℓ, the conservation of parity must be taken into account.

The form factor, F -- which for a stripping reaction is simply the Fourier transform of the wave function of the incoming particle, and for other types of direct interaction a complicated function of the wave functions involved -- determines the particular type of direct interaction under study. The particular spherical Bessel function chosen is determined only by the initial and final spins and parities, and it offers no information as to the exact form of interaction taking place.

Several approximations are involved in the derivation of the Butler expression:[36]

(a) the interaction takes place only with the captured nucleon, which means that the incoming nuclide can be thought to exist in a configuration f + c, where f is the final escaping particle and c is the captured one. Condition (a) also implies that the distance between f and c is large.

(b) Coulomb effects are neglected. For the validity of this approximation it is necessary that the energy of the projectile be greater than Ze^2/r, where Z is the charge of the target nucleus, e the unit of charge.

(c) Nuclear interactions with the whole bombarding nucleus are ignored; the condition necessary for the validity of this approximation is that the projectile should have an energy greater than $\hbar^2/2mr^2$, where m is the mass of the bombarding particle.

(d) Nuclear interactions with the outgoing particles are ignored, and finally,

(e) Compound nucleus effects are neglected.

Butler's theory was fairly successful[19,50,55,69,70] in predicting the peak positions in the angular distributions of direct-interaction processes, and soon other workers attempted to modify it by taking into account several of the neglected factors,[71-77] with some degree of success.

Angular Distributions from $Al^{27}(\alpha,t)Si^{28}$ and $Fe^{56}(\alpha,t)Co^{57}$

The success of the theory was the factor that motivated a trial at fitting the angular distributions of tritons from the (α,t) reaction with a Butler treatment.

The angular distributions of the tritons from the two reactions investigated clearly indicated their origin from direct-interaction processes because of the strong forward peaking and the high energy of the tritons.

It was not possible to use a theoretical form factor because the wave function for the helium ion is not known; instead recourse was taken to the device originated by Hunting and Wall,[55] which was to use a function $\exp(-|3/4\ \vec{k}_i - \vec{k}_f|^2/Q_o^2)$ as the form factor, where Q_o^2 is taken as an adjustable parameter. By doing this, of course, one abandons any hope of determining the mechanism of the reaction by the study of the angular distribution, since the real functional form of the form factor is unknown. A separate plot of the form factor and the spherical Bessel function used for the $Fe^{56}(\alpha,t)Co^{57}$ fit is shown in Fig. 27.

Figures 21 and 22 show the fitting of the differential cross-section data for the $Al^{27}(\alpha,t)Si^{28}$ reactions with a Butler treatment. The best fit seems to be for radii of 5.50 and 5.65 x 10^{-13} cm for reactions leading to the ground state and first excited state of Si^{28} respectively. The radius of the aluminum nucleus is 4.2 x 10^{-13} cm (using a radius parameter of 1.4 x 10^{-13} cm) and that of the helium ion is 1.2 x 10^{-13} cm,[35] giving a total contact radius of 5.4 x 10^{-13} cm. In both cases the peaks and shoulders in the experimental angular distributions coincide with the peaks of the theoretical curve. The ℓ values chosen for the spherical Bessel function were 2 for the groundstate transition and 0 for the first-excited-state transitions, in accordance

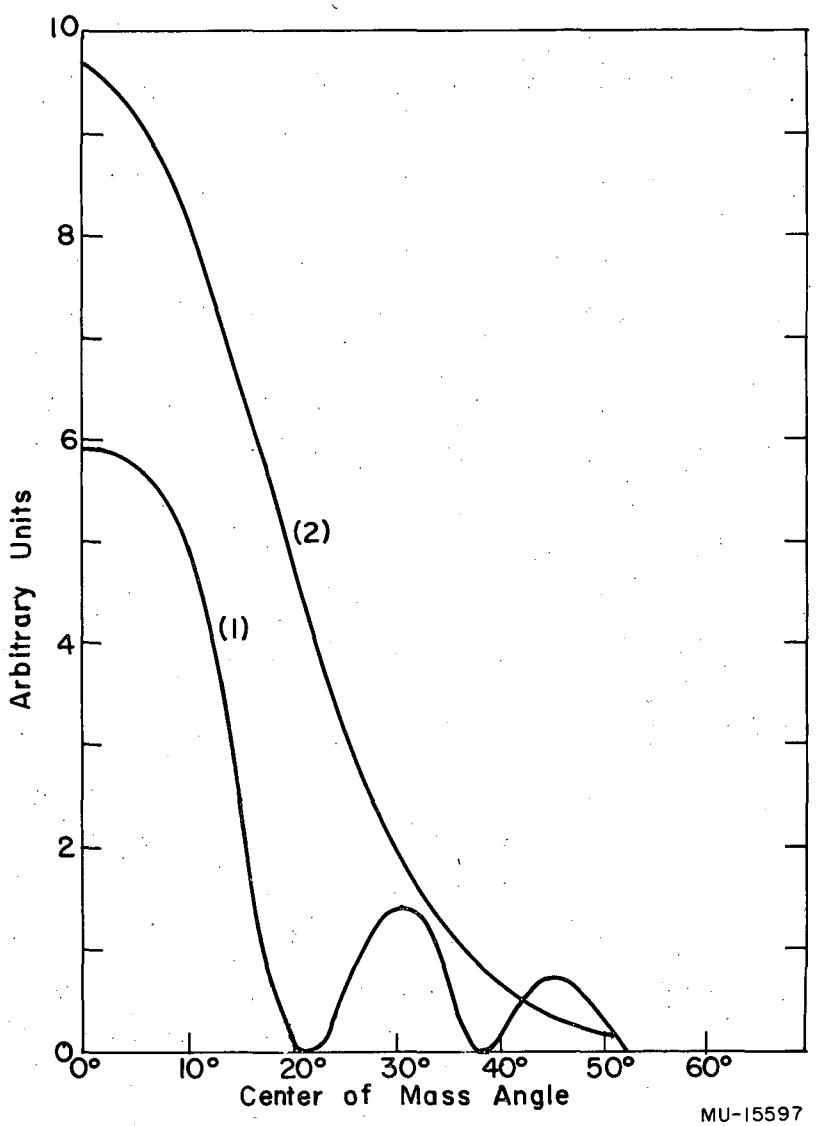

Fig. 27. Functions used for the Butler fitting of the triton angular distribution arising from the $Fe^{56}(\alpha,t)Co^{57}$ reaction.
Curve (I) is the spherical Bessel function $\left|j_{7/2}\,(qr)\right|^2$
Curve (2) is the form factor for the reaction
$\left|F_d\right|^2 = e^{-\left|3/4\,\vec{k}_o - \vec{k}_f\right|^2/Q_o^2}$ with $Q_o^2 = 1.34 \times 10^{26}\ cm^{-1}$.

with Butler's theory, since the ground state of Al^{27} is 5/2+ and the ground state and first excited states of Si^{28} are 0+ and 2+.

Figure 23 shows the same type of data for the $Fe^{56}(\alpha,t)Co^{57}$ reaction. Again the general agreement between the experimental curve and the theoretical curve is rather good. The radius of interaction obtained from the Butler curve is 5.85×10^{-13} cm. The radius of the Fe^{56} nucleus is 4.6×10^{-13} cm (using 1.2×10^{-13} cm as the radius parameter), so that the total radius is 5.8×10^{-13} cm. The ℓ chosen for the fit was 3, again in agreement with the Butler's theory prediction for a transition from the ground state of Fe^{56} (0+) to the ground state of Co^{57} (7/2-).

The detailed agreement between the shapes of the experimental and theoretical angular distributions, however, is not too good. The reasons for this disagreement are many. The most important is that the helium ion cannot be considered as a loosely bound structure, so that the nuclear approximations do not hold valid in this case. Another cause for disagreement is that for a doubly charged particle Coulomb effects are rather important. Both these factors tend to fill in the valleys between the peaks of the theoretical distribution, besides tending to broaden and shifting the peaks.[36]

The experimental cross-section is much greater at large angles than the theoretical treatment would allow. This seems to be a general failing of the Butler theory.[78] Several theories have been put forward to explain this effect. Some try to combine Butler's distributions with compound-nucleus angular distributions and the corresponding interference terms.[79] Others have antisymmetrized the total wave function of the direct-interaction process (which Butler neglected to do) in various ways and tried to explain the large-angle cross sections by having a share of the emitted particles coming from the target nucleus with an angular distribution peaked in the backward direction.[78,80-83] At this point, however, the theories are still in a state of flux.

The integrated cross-sections from the angular distributions have already been given. They seem to account for a large part of the total cross-section, showing again the importance of the direct-interaction process in the (α,t) reactions.

CONCLUSIONS

It has been proven that almost all the $(\alpha,p2n)$ cross-section in the heavy elements is really produced by an (α,t) reaction. These tritons are the product of a direct interaction, very possibly a stripping process, and have large energies in consequence.

Studies of the (p,t), (d,t), and (α,t) reactions through the periodic table have shown similarities between these processes, namely strong contributions from both (a) the compound-nucleus mechanism, and (b) from the direct-interaction mechanism at low Z. The compound-nucleus contribution fades away at large Z, leaving the reaction to proceed almost entirely by direct interactions.

It has been shown that a single and a double pickup are probable mechanisms for the (d,t) and (p,t) reactions.

It has also been shown that the data from angular distributions of (α,t) reactions are in agreement with the information derived from the cross-section work. Finally, it was demonstrated that Butler's theory gives a surprisingly good fit to these angular distributions.

ACKNOWLEDGMENTS

I would like to acknowledge the guidance and continued interest of Professor Glenn T. Seaborg.

I would also like to thank Dr. William H. Wade for his help and guidance during the entire project.

I am pleased to thank Dr. Bernard G. Harvey for many helpful discussions, Dr. Paul F. Donovan for many enjoyable arguments, and Dr. Bruce M. Foreman and Dr. Richard A. Glass for their cooperation.

I also like to extend my thanks to Dr. Homer Conzett, Harlan Shaw, and George Merkel for their help with the scattering chamber techniques.

Appreciation is expressed to Dr. Floyd Momyer for advice during calibration of the counting equipment and George Shalimoff for performing the spectroscopic analysis of the metals.

I would like to express my gratitude to W. Barclay Jones, Peter McWalters, J. Woods, and R. Cox, and other members of the Crocker Laboratory 60-inch cyclotron crew, as well as to the crew of the 32-Mev linear accelerator, who have been very coöperative.

This work was performed under the auspices of the United States Atomic Energy Commission.

REFERENCES

1. Bruce M. Foreman, Jr., Spallation and Fission Competition in Thorium-232 and the Masses of the Heaviest Elements (thesis), UCRL-8223, April 1958.

2. T. Darrah Thomas, Spallation Fission Competition from the Compound System U^{233} plus He^{4} (thesis), UCRL-3791, July 1957.

3. Robert Vandenbosch, Fission and Spallation Competition in Ra^{226}, Th^{230}, U^{235}, and Np^{237} (thesis), UCRL-3858, July 1957.

4. R. Vandenbosch, T. D. Thomas, S. Vandenbosch, R. A. Glass, and G. T. Seaborg, Phys. Rev. (to be published).

5. S. E. Ritsema, Fission and Spallation Excitation Functions of U^{238} (thesis), UCRL-3266, Jan. 1956.

6. Glass, Carr, Cobble, and Seaborg, Phys. Rev. 104, 434 (1956).

7. Robert J. Carr, Spallation-Fission Competition in the Nuclear Reactions of Plutonium Induced by Alpha Particles (thesis), UCRL-3395, April 1956.

8. W. John, Jr., Phys. Rev. 103, 704 (1956).

9. F. N. Spiess, Phys. Rev. 94, 1292 (1954).

10. Templeton, Howland, and Perlman, Phys. Rev. 72, 758, 766 (1947).

11. L. Evan Bailey, Angle and Energy Distribution of Charged Particles from the High-Energy Nuclear Bombardment of Various Elements (thesis), UCRL-3334, March 1956.

12. W. H. Barkas and H. Tyren, Phys. Rev. 89, 1 (1953).

13. R. Deutsch, Phys. Rev. 97, 1110 (1955).

14. Currie, Libby, and Wolfgang, Phys. Rev. 101, 1557 (1956).

15. B. L. Cohen and T. H. Handley, Phys. Rev. 93, 514 (1954).

16. J. R. Holt and T. N. Marsham, Proc. Phys. Soc. (London) 66A, 1032 (1953).

17. J. B. Marion and G. Weber, Phys. Rev. 102, 1355 (1956).

18. I. Resnick and S. S. Hanna, Phys. Rev. 82, 463 (1951).

19. J. A. Harvey, Can. J. Phys. 31, 278 (1953).

20. N. V. Sidgwick, The Chemical Elements and their Compounds (Oxford University Press, Oxford, England, 1951).

21. Hollander, Perlman, and Seaborg, Revs. Modern Phys. 25, 469 (1953).

22. R. L. Wolfgang and W. F. Libby, Phys. Rev. 85, 437 (1952).

23. Robert E. Ellis, Elastic Scattering of 48-Mev Alpha Particles by Heavy Nuclei (thesis), UCRL-3114, Aug. 1955.

24. R. E. Ellis and L. Schecter, Phys. Rev. 101, 636 (1956).

25. Gerhard E. Fischer, The Scattering of 10-Mev Protons on Carbon and Magnesium (thesis), UCRL-2546, 1954.

26. G. E. Fischer, Phys. Rev. 96, 704 (1954).

27. Robert G. Summers-Gill, Some Properties of the Beryllium Nucleus Obtained from Scattering Data (thesis), UCRL-3388, April 1956.

28. R. G. Summers-Gill, Phys. Rev. 109, 1591 (1958).

29. Franklin J. Vaughn, Elastic and Inelastic Scattering of 48-Mev Alpha Particles by Carbon and Magnesium, UCRL-3174, Oct. 1955.

30. Harrold Brook Knowles, The Differential Cross Sections of the Alpha Particles from Carbon Induced by 31.8-Mev Protons (thesis) UCRL-3753, April 1957.

31. E. B. Paul and R. L. Clark, Can. J. Phys. 31, 267 (1953).

32. H. A. Bethe, Revs. Modern Phys. 9, 161 (1937).

33. B. L. Cohen, Phys. Rev. 80, 105 (1950).

34. K. J. LeCouteur, Proc. Phy. Soc. (London) A63, 259 (1950).

35. J. M. Blatt and V. F. Weisskopf, Theoretical Nuclear Physics (Wiley, New York, 1952).

36. S. T. Butler and O. H. Hittmair, Nuclear Stripping Reactions (Wiley, New York, 1957).

37. R. Huby, review article on "Stripping Reactions", in Progress in Nuclear Physics, Vol. 3 (Butterworth-Springer Ltd., London, 1954).

38. R. Serber, Phys. Rev. 72, 1008 (1947).

39. R. Serber, Phys. Rev. 72, 1114 (1947).

40. D. N. Kundu and M. L. Pool, Phys. Rev 73, 22 (1948).

41. D. C. Peaslee, Phys. Rev. 74, 1001 (1948).

42. H. C. Newns, Proc. Roy. Soc. (London) A65, 916 (1952).

43. Bailey, Freier, and Williams, Phys. Rev. 73, 274 (1948).

44. Borner, Eisinger, Kraus, and Marion, Phys. Rev. 101, 209 (1956).

45. Holmgreen, Blair, Simmons, Stratton, and Stuart, Phys. Rev. 95, 1544 (1954).

46. Bonner, Evans, Harris, and Phillips, Phys. Rev. 80, 164 (1950).

47. McEllistran, Chibam Douglas, Herring, and Silverstein, Phys. Rev. 99, 632(A) (1955).

48. Bennett, Bonner, Hudspeth, Richards, and Watt, Phys. Rev. 59, 781 (1941).

49. Bonner, Evans, Harris, and Phillips, Phys. Rev. 75, 1401 (1949).

50. W. F. Vogelsang and J. N. McGruer, Phys. Rev. 109, 1663 (1958).

51. J. B. Marion and G. Weber, Phys. Rev. 102, 1355 (1956).

52. I. Resnick and S. S. Hanna, Phys. Rev. 82, 463 (1951).

53. L. Eisenbud and E. P. Wigner, Nuclear Structure (Princeton University Press, Princeton, 1958).

54. Wade, Gonzalez-Vidal, Glass, and Seaborg, Phys. Rev. 107, 1311 (1957).

55. C. E. Hunting and N. S. Wall, Phys. Rev. (to be published).

56. Blatt and Biedenharn, Revs. Modern Phys. 24, 258 (1952).

57. L. Wolfenstein, Phys. Rev. 82, 690 (1951).

58. S. T. Butler, Phys. Rev. 80, 1095 (1950).

59. S. T. Butler, Proc. Roy. Soc. (London) A208, 559 (1951).

60. S. T. Butler, Phys. Rev. 107, 272 (1957).

61. S. T. Butler, Phys. Rev. 88, 685 (1952).

62. S. T. Butler and H. A. Bethe, Phys. Rev. 85, 1045 (1952).

63. Parkinson, Beach, and King, Phys. Rev. 87, 387 (1952).

64. King and Parkinson, Phys. Rev. 88, 141 (1952).

65. S. T. Butler and E. E. Salpeter, Phys. Rev. 88, 133 (1952).

66. Austern, Butler, and McManus, Phys. Rev. 92, 350 (1953).

67. Bathia, Huang, Huby, and Newns, Phil. Mag. 43, 485 (1952).

68. Daitch and French, Phys. Rev. 87, 900 (1952).

69. H. B. Burrows, Phys. Rev. 80, 1095 (1950).

70. C. E. Dickerman, Phys. Rev. 109, 443 (1958).

71. E. Gerjuoy, Phys. Rev. 91, 645 (1953).

72. F. L. Friedman and W. Tobocman, Phys. Rev. 92, 93 (1953).

73. S. T. Butler and N. Austern, Phys. Rev. 93, 355 (1954).

74. I. P. Grant, Proc. Roy. Soc. (London) 67, 981 (1954).

75. I. P. Grant, Proc. Roy. Soc. (London) 68, 244 (1955).

76. W. W. Pratt, Phys. Rev. 97, 131 (1955).

77. W. Tobocman and M. Kalos, Phys. Rev. 97, 132 (1955).

78. A. P. French, Phys. Rev. 107, 1655 (1957).

79. R. G. Thomas, Phys. Rev. 100, 25 (1955).

80. N. T. Evans and A. P. French, Phys. Rev. 109, 1272 (1957).

81. G. E. Owen and L. Madansky, Phys. Rev. 105, 1766 (1957).

82. L. Madansky and G. E. Owen, Phys. Rev. 99, 1608 (1955).

83. J. C. Hansel and W. C. Parkinson, Phys. Rev. 110, 128 (1958).